applied sciences

MDPI

Article

Deployment Optimization of Defense Stations in an Attack-Defense Aerial War Game

Zhi-Xiang Jia † and Jean-Fu Kiang *,†

Graduate Institute of Communication Engineering, National Taiwan University, Taipei 10617, Taiwan
* Correspondence: jfkiang@ntu.edu.tw; Tel.: +886-2-33663661
† These authors contributed equally to this work.

Abstract: An attack–defense aerial war game is developed to maximize the capability of defense forces in protecting a target area from an attack force. The attack force is composed of multiple attack stations in slant or pincer formation, and each attack station can launch multiple attackers against the defense force. The defense force is composed of one major post, two minor posts, and multiple defense stations, and each defense station is equipped with multiple interceptors against the approaching attackers. Four optional defense goals are proposed to guide the deployment of defense stations. A particle swarm optimization (PSO) algorithm is applied to acquire an optimal deployment plan of all the defense stations, under a specific defense goal. Multiple games are played with the optimal deployment plan, and the results are analyzed statistically. Interesting outlier cases are also inspected to gain more insights on the nature of the games.

Keywords: aerial war game; attack; defense; route planning; deployment; particle swarm optimization (PSO)

check for updates

Citation: Jia, Z.-X.; Kiang, J.-F. Deployment Optimization of Defense Stations in an Attack-Defense Aerial War Game. *Appl. Sci.* **2022**, *12*, 10801. https://doi.org/10.3390/app122110801

Academic Editor: Giancarlo Mauri

Received: 7 September 2022
Accepted: 20 October 2022
Published: 25 October 2022

1. Introduction

War games have been widely used to gain insights and lessons from a wide variety of scenarios that are otherwise improbable to observe without playing the games. Useful information like critical factors and effective strategy manifested in the games can help reduce the risk in real lives. In this work, an attack–defense aerial war game is developed to maximize the capability of defense force in protecting a target area from an attack force and gain some insights on the nature of the games.

A typical aerial war game is staged in a specific scenario and proceed in various constituent episodes. The players in a game try to achieve their own goal by using specific methods or techniques, and follow predefined game rules in conducting each episode. For example, in [1], a cooperative combat between two teams of unmanned aerial vehicles (UAVs) was simulated. Three training techniques were proposed to enhance the performance of a multi-agent deep Q-learning (MADQN) method. A scenario–transfer training was exercised in a simple task, a self-play training was used to iteratively improve the performance of UAVs in a team, and a rule-coupled training was embedded in the combat rules to constrain the exploration space. However, some practical factors such as kill probability and maximum flying distance were not considered. In [2], an air combat between two UAVs was modeled as an optimization problem, and a moving-time horizon scheme was proposed to search for the optimal trajectories of UAVs. In [3], two opponent UAVs competed to fire missiles against each other by applying a deep learning method to choose an optimal maneuver angle, based on the predicted state and a decision objective function. The proposed method was claimed to be more flexible in decision-making and more economic in computational time than some previous works. Similar conflicts between two forces of same size and composition were also studied [1–3]. In this work, an aerial war game is developed between an attack force and a defense force of comparable capabilities.

There are many episodes that involve three players. For example, in [4], a (TAD) game was developed, with an attacker pursuing a moving target while evading a defender. The moving target cooperated with the defender, and the attacker switched role between pursuer and evader. In [5], an active target defense differential game (ATDDG) was proposed, in which a missile (attacker) tracked an aircraft (target) and the latter fired a defense missile (interceptor) against the former. A closed-form solution of the ATDDG was implemented as a state-feedback controller for the target and the interceptor, aiming to increase the opportunity of target survival. The attacker and the interceptor flew at the same speed, the guidance rules of the attacker were unknown, and the escape scheme of attacker was not mentioned. In [6], an active target–attacker–defender (ATAD) differential game involved an attacker, multiple targets, and a defender. The attacker aimed at the closest target, and the defender protected the targets or intercepted the attacker. The interaction between agents was modeled as a linear quadratic differential game (LQDG), reaching an open-loop Nash equilibrium. The agents could change their strategies by taking a receding horizon approach to compute their trajectories accordingly. Interception is a common practice to protect targets from attackers [4–6], which is also incorporated in our aerial war game.

Some coordination is required when multiple players are involved in a game scenario. For example, in [7], multiple fighters were dispatched to suppress an integrated air defense system (IADS). An improved chaotic particle swarm optimization (I-CPSO) algorithm was applied on both sides. The simulations included consumption of air-to-air missiles, distance to non-escape zone and jamming distance, but the efficacy of the dispatch plan was not verified. In [8], a beyond-visual-range (BVR) air combat between two fleets of UAVs was formulated as a cooperative decision-making problem. Both fleets competed to maximize the difference between predominance and threat in terms of relative distance and relative height. A zero-sum matrix game was developed by using a double oracle and neighborhood search (DO-NS) algorithm. Aerial war games were also played to improve the tactical operations. In [9], an optimization procedure was proposed to fire missiles against high-velocity attackers, which incorporated practical factors such as multiple phases (initial, midcourse, and terminal) of attackers, multiple targets, interceptor cost, interceptor kill probability, detection probability of attackers, and risk attitude (human psychological features under stress) of the defender. Combinatorial mathematics was applied to model multiple phases and multiple targets, and a cumulative prospect theory (CPT) was used to model the risk attitude of the defender. The assignment plan of interceptors was acquired, but its efficacy was not verified by simulations. In [10], a static multi-objective weapon-target assignment (SMWTA) algorithm was proposed to assess combat condition, based on the damage to opponent, cost of missiles, and loss of fighting capacity inflicted by an opponent counterattack. A non-dominated sorting genetic algorithm III (NSGA-III) was applied to search for Pareto solutions in the decision space. An assignment plan of fighters and missiles to targets was obtained, but its efficacy was not verified. The fighting capacity was counted in terms of the fighter value, the target value, and the launch range of missiles, but some practical factors such as escape capability of fighters and kill probability against moving object were not considered. Better assignment plan of agents can inflict more serious wreck on the enemy force [7–10], which is also included in our work.

Evading maneuvers has been implemented in aerial war games. For example, in [11], two homing missiles shared their measured line-of-sight (LoS) with each other to improve their tracking performance on an aerial target. A blinding-evasion guidance law was proposed to confuse the two homing missiles, and an evasive maneuver was taken to increase the target survivability.

Defense on a border or a territory has been a popular theme of war games. In [12], a strategy based on dominant region was proposed for multiple defenders to intercept an intruder before it entered a target area. The game highlighted the approaching method of intruder and the interception method of defenders. The intruder maneuvered in response to the defenders' strategies instead of following a premeditated plan. In [13], a reach–avoid

perimeter defense game was played between intruders and defenders. Multiple intruders were sent to the target area, and the defenders deployed around the target perimeter would strike the intruders with a cooperative defense strategy. In [14], a border defense scenario was studied, where two intruders sneaked as close to the border as possible and an UAV would try to capture these intruders as far away from the border as possible. A differential game was formed to search for the optimal motions of the UAV and the cooperative intruders, respectively. In [15], evolution strategies (ES) were applied to a team of fixed-wing planes in attacking an enemy base station while avoiding its guarding quadcopters. The strategies were also applied to two teams, equipped with the same number of planes and base stations, operating on different policies to defeat the opponent planes or attack the opponent base stations. The aerial war game in our work is staged to protect a specific area with multiple defense stations, similar to [12–15], but the area size and the number of agents are increased to inspect some nuances aroused by the complicated game scenario.

Maneuvering of attackers and defenders directly determines the outcome of their engagement. In [16], a reinforcement learning (RL) algorithm through amplification of imitation effect (AIE) was proposed to enhance the capability of single or multiple combat unmanned aerial vehicles (CUAVs) in pursuing a target while evading missiles fired from the latter. A self-imitation learning (SIL) algorithm based on the best previous decision and a random network distillation (RND) algorithm were used to guide the exploration. However, the kill probability of UAV or missile was not considered in these works. In [17], an all-domain simulation (ACS) was proposed to dispatch a group of UAVs (attackers), without path planning or map navigation, to attack multiple static targets while bypassing the area covered by radar stations (defenders). Each target was marked by only one attacker, the targets were located outside of the radar coverage area, and no interceptors were fired against the attackers. In [18], a virtual target approach was proposed to guide a missile to hit a static target or a target moving at constant speed. A missile was first planned to hit a virtual target at a given impact angle by following a nonsingular terminal sliding-mode guidance law. Then, the missile flew at a fixed angle to the real target by following a proportional navigation guidance (PNG) law. An optimization algorithm was applied to simultaneously control the impact time and angle on the real target. In comparison, our work aims to search an optimal deployment plan of defense stations, and the interceptors in the air maneuver by specific rules to cope with the attackers on the move.

Chasing episodes between pursuer(s) and evader(s) are indispensable ingredients in a complicated game scenario. In [19], a pursuit–evasion differential game was studied, with multiple attackers trying to capture a moving target armed with no interceptor. Time-varying optimal control algorithms were developed for both attackers and target, with limited on-site information. Some attackers might lure the target to a region for the other attackers to capture it off guard. In [20], a pursuit-evasion differential game was played between three pursuers and an evader. The strategies for all the agents were derived with a geometric method, which could be extended to involve more pursuers. The chasing episodes together with imperfect kill probability sometimes may turn the tide of a game, which will be demonstrated with some interesting cases in this work.

Most works in the literature highlighted a few factors of interest to assess their effects. By combining more practical factors into the scenario, the game may become closer to real-life operations, manifesting some nuances that will otherwise be missing in the lack of interaction among different factors.

In this work, an aerial war game between an attack force and a defense force is developed, aiming to find an optimal deployment plan of defense stations for the protection of the defense force. The attack force is composed of multiple attack stations in slant formation or pincer formation, with each station equipped with multiple attackers. The defense force is composed of three commanding posts and multiple defense stations, with each station armed with multiple interceptors against the approaching attackers. A particle swarm optimization (PSO) algorithm is applied to find the optimal deployment plan of defense stations, based on four possible options of defense cost. Multiple games are then

played on the optimal deployment plan, and the feasibility of the plan is evaluated by the statistics on the simulation results.

The rest of this work is organized as follows: The game design is presented in Section 2, the simulation results and statistical analysis are presented in Section 3, some interesting outlier cases are reviewed in Section 4, simulation results with perfect kill probability are discussed in Section 5, comparisons and further discussions are presented in Section 6, empirical deployment plans are proposed and simulated in Section 7, and some conclusions are drawn in Section 8.

2. Game Design

In this work, an attack–defense aerial war game is developed. More practical factors than typically found in the literature are incorporated to make the scenario closer to real-life combat. The scenario includes episodes of target assignment, attack, interception, evading, defense, and pursuer chasing evader. In the following subsections, we will sequentially elaborate formation of attack stations, route planning of attackers, engagement of attacker and interceptor, attacker maneuverability, deployment of defense stations, defense cost function, and default parameters used in the simulations.

2.1. Formation of Attack Stations

Figure 1 shows a slant formation and a pincer formation, respectively, of attack stations deployed in the simulations. By taking a slant formation, the north attack stations are closer to the target area than the south attack stations. In traditional warfares, the south attack stations may keep alert and cover the north attack stations in case of retreat. The former may join the operation if the latter proceed as planned. However, in an all-out assault, the south attack stations may lose some edge because of farther distance from their targets. By taking a pincer formation, both north and south attack stations will exert higher pressure on the defense force if salvo action is taken. The downside is higher risk in retreating if the defense force counterattacks effectively.

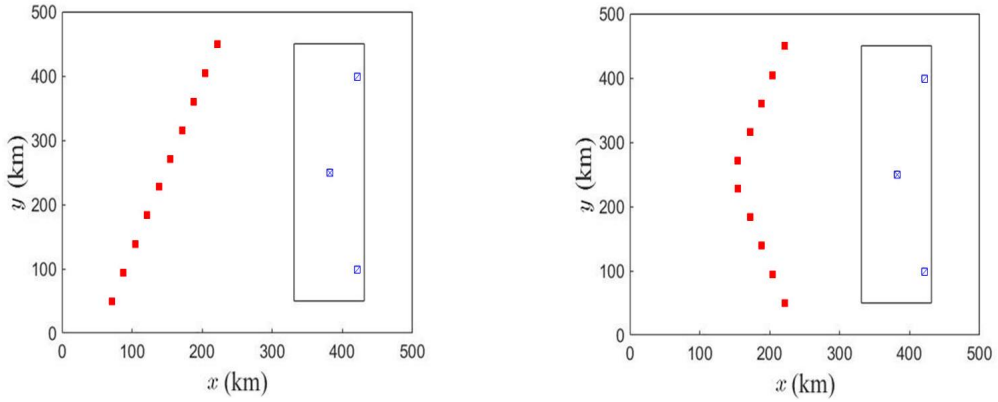

Figure 1. Attack stations in (**a**) slant formation; (**b**) pincer formation.

2.2. Route Planning of Attackers

Figure 2 shows an exemplary game scenario in this work. The attack force is composed of multiple attack stations in slant formation or pincer formation, with each station equipped with multiple attackers. The defense force is composed of three commanding posts and multiple defense stations, with each station armed with multiple interceptors against the approaching attackers. More than 100 agents are engaged over an area of 500 km $\times$ 500 km, including a protected territory of 100 km $\times$ 400 km.

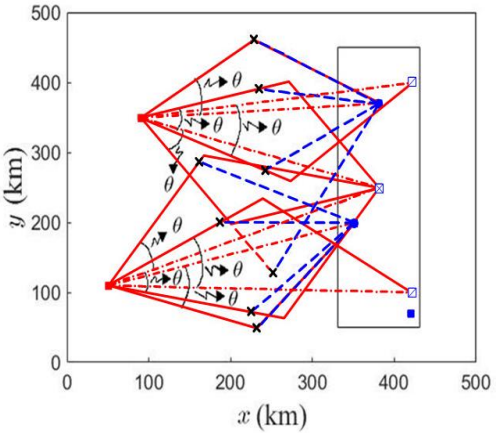

Figure 2. Exemplary scenario of route planning, square with cross: major post, square with slash: minor post, blue square: defense station, red square: attack station, ———: planned attacker path, ×: anticipated intercept point, − − −: anticipated attacker path, − − −: anticipated interceptor path, − · −: target assignment of attack station, rectangular frame: deployment area of defense stations.

Each attack station plans two diverse paths to the major post, one path to the nearer minor post, and one path to the nearest defense station. Two attackers are dispatched to the major post from the left and the right flanks, respectively, at an angle θ about a straight line connecting the major post and the attack station, then detour for the major post at the middle point. An attacker aiming for the north (minor) post will approach from the right flank, and that aiming for the south (minor) post will approach from the left flank. The attacker aiming for the nearest defense station will approach from the flank farther from the major post.

2.3. Engagement of Attacker and Interceptor

If an attacker A_m flies within the coverage area of some defense station, the latter will fire an interceptor B_n on A_m. If A_m is marked by only one interceptor and is within 50 km of its target, a defense station within 40 km of the target will fire another interceptor on A_m. A targeted defense station may fire another interceptor on A_m by itself. At each simulation time step, the defense force computes an achievable intercept time, t_h, for B_n (at Q_n) to hit A_m (at P_m) by solving

$$|P_m + \bar{U}_{am} t_h - Q_n| - v_b t_h = 0, \;\; 0 < t_h \leq 1000 \tag{1}$$

where $\bar{U}_{am}$ is the velocity vector of A_m and v_b is the interceptor speed. If no intercept time is found, the interceptor will tailgate A_m. If A_m no longer exists, B_n will detour for the nearest attacker.

At each time step, each attacker will check if it is marked by any interceptor. If an interceptor B_n (at Q_n) appears within alert radius R_a of attacker A_m (at P_m), the attack force computes an anticipated intercept time, t_h, by solving

$$|(P_m + \bar{U}_{am} t_h) - (Q_n + \bar{U}_{bn} t_h)| = 0, \;\; 0 < t_h \leq 1000 \tag{2}$$

where $\bar{U}_{bn}$ is the velocity vector of B_n.

An attacker vanishes if it runs out of fuel or gets hit by an interceptor. An attacker hits its target if their separation distance is shorter than the impact radius D_a of the attacker. An interceptor is lost if it runs out of fuel or hits an attacker. An interceptor hits an attacker with kill probability p_k if the latter falls within the impact radius D_b of the interceptor.

In this work, assume all the attackers and interceptors fly at the same speed, and an attacker has certain maneuverability to evade an interceptor. When interceptor B_n (at Q_n) appears within an alert radius R_a of attacker A_m (at P_m), the attack force will compute an

intercept time by solving (2). If an intercept time is found, A_m will evade B_n by adjusting its velocity vector as

$$\bar{U}_{am} = v_a \frac{\alpha_e \hat{u}\{Q_n X_m\} + (1-\alpha_e)\hat{u}\{P_m X_m\}}{|\alpha_e \hat{u}\{Q_n X_m\} + (1-\alpha_e)\hat{u}\{P_m X_m\}|} \tag{3}$$

where v_a is the attacker speed, α_e is the attacker maneuverability, with $0 \leq \alpha_e \leq 1$, X_m is the anticipated intercept point, $\hat{u}\{Q_n X_m\}$ is the unit vector of $\overline{Q_n X_m}$, and $\hat{u}\{P_m X_m\}$ is the unit vector of $\overline{P_m X_m}$. Attacker A_m will regularly adjust its velocity vector as long as B_n remains within its alert radius and an intercept point is found. If intercept point no longer exists, B_n will tailgate A_m, and A_m will fly for its assigned target via a straight path. Interceptor B_n will track A_m via a straight path if an intercept point emerges again. Otherwise, B_n will tailgate A_m and may not be able to catch the latter since they fly at the same speed.

If A_m is marked by more than one interceptors, it will detour for the nearest defense station or post via a straight path. If the defense station originally targeted by A_m has been hit, A_m will detour for the nearest defense station or post via a straight path.

Each defense station is composed of a radar unit and a few interceptor launching units at safe distance from the radar. Assume that the attackers only aim for the radar unit; hence, a defense station being hit means that the radar unit is lost and no more interceptors can be fired. The remaining interceptors will not be counted in the defense cost at the end of the game.

2.4. Attacker Maneuverability

Figure 3 shows the simulated attacker lost rate versus attacker maneuverability α_e, with the kill probability of interceptor, $p_k = 0.6$ and 0.7, respectively. The attacker lost rate is defined as

$$A_c = 100 \times \frac{M_c}{M_0}\% \tag{4}$$

where M_c is the number of attackers hit by interceptors, and M_0 is the total number of attackers dispatched in one game. At a given α_e, 200 games are played, with the defense stations randomly distributed in the deployment area. It is observed that A_c has a minimum value at $\alpha_e = 0.5$, and the value of A_c at $p_k = 0.6$ is lower than its counterpart at $p_k = 0.7$. Larger α_e implies an attacker may turn sidewise or even backwards to evade an interceptor. Once the intercept point is lost, the attacker will resume its original target via a straight path. The interceptor may capture the attacker on its resumed course later.

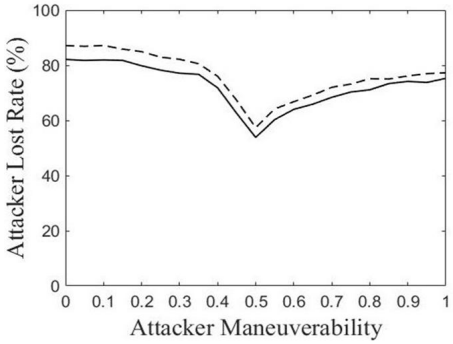

Figure 3. Attacker lost rate versus maneuverability, ———: $p_k = 0.6$, − − −: $p_k = 0.7$.

2.5. Deployment of Defense Stations

Multiple attackers are dispatched from attack stations to strike the commanding posts and the defense stations via planned routes. Imperfect kill probability of interceptors, maneuverability of attackers for evading interception, and the maximum flight range of attackers and interceptors are implemented in the game. Due to the complexity of

the game, exacerbated by the imperfect kill probability, it is difficult to apply analytical approaches to find the optimal deployment plan of defense stations. In this work, a particle swarm optimization (PSO) algorithm [21], reputed for fast convergence, is applied to find the optimal deployment plan of defense stations, by minimizing a specific defense cost function ζ_α.

A set of N particles are used to represent the candidate coordinates of M defense stations, with the position of the nth particle given by $\bar{S}_n = (S_{n1x}, S_{n1y}, S_{n2x}, S_{n2y}, \cdots, S_{nMx}, S_{nMy})$, where (S_{nmx}, S_{nmy}) are the coordinates of the mth defense station. Similarly, the velocity of the nth particle is given by $\bar{V}_n = (V_{n1x}, V_{n1y}, V_{n2x}, V_{n2y}, \cdots, V_{nMx}, V_{nMy})$. In the beginning, the position and velocity of each particle are randomly selected from given intervals as

$$x_{\min} \le S_{nmx} \le x_{\max} \tag{5}$$

$$y_{\min} \le S_{nmy} \le y_{\max} \tag{6}$$

$$V_{x,\min} \le V_{nmx} \le V_{x,\max} \tag{7}$$

$$V_{y,\min} \le V_{nmy} \le V_{y,\max} \tag{8}$$

with $1 \le n \le N$ and $1 \le m \le M$.

The position of the nth particle is used to deploy the M defense stations and a game is played accordingly, resulting in a defense cost function $\zeta_{\alpha n}$. If $\zeta_{\alpha n}$ is lower than the lowest defense cost in previous iterations, the best defense cost is updated as $\zeta'_{\alpha n} = \zeta_{\alpha n}$, and the best position is updated as $\bar{S}_{bn} = \bar{S}_n$. The lowest defense cost among all the N particles iterated so far is recorded as the global best defense cost, $\zeta_{\alpha g}$, and the associated particle position is recorded as the global best position, $\bar{S}_g$.

In the next iteration, the velocity of the nth particle is updated as

$$\bar{V}_n \leftarrow w_v \bar{V}_n + c_1 r_1 (\bar{S}_{bn} - \bar{S}_n) + c_2 r_2 (\bar{S}_g - \bar{S}_n) \tag{9}$$

where w_v is a weight on particle velocity, c_1 and c_2 are acceleration constants, r_1 and r_2 are uniform random numbers over $[0, 1]$. The updated velocity components are constrained within the given intervals. If $V_{nm\alpha} > V_{\alpha,\max}$, then set $V_{nm\alpha} = V_{\alpha,\max}$, with $\alpha = x, y$. Similarly, if $V_{nm\alpha} < V_{\alpha,\min}$, then set $V_{nm\alpha} = V_{\alpha,\min}$, with $\alpha = x, y$. Next, the position of the nth particle is updated as

$$\bar{S}_n \leftarrow \bar{S}_n + \bar{V}_n \tag{10}$$

The updated position is constrained by reflection boundary conditions. If $S_{nm\alpha} > \alpha_{\max}$, then $S_{nm\alpha} \leftarrow 2\alpha_{\max} - S_{nm\alpha}$, with $\alpha = x, y$. Similarly, if $S_{nm\alpha} < \alpha_{\min}$, then $S_{nm\alpha} \leftarrow 2\alpha_{\min} - S_{nm\alpha}$, with $\alpha = x, y$. The updated position $\bar{S}_n$ is then used to play another game. The global best position $\bar{S}_g$ after a given number of iterations will be used as the optimal deployment plan of all the defense stations.

In [22], a multi-agent decision support system (DSS), including missile, radar, and command center, was established for missile defense. The objective function of DSS counted in the constraints of radar, offensive missile, intercept missile, and commander. A variable neighborhood negative selection particle swarm optimization (VNNSPSO) algorithm was proposed to obtain an optimal interception plan dynamically. The proposed algorithm was verified by comparing with basic PSO and several variants in terms of convergence rate, iteration number, average fitness value, and standard deviation.

In [23], an adaptive simulated annealing-particle swarm optimization (SA-PSO) algorithm was proposed to optimize the relative distances and angles of a leader and its follower missiles in a cooperative multi-missile formation to attain combat effectiveness. The formation was optimized to accomplish different missions. An evaluation index system was designed for the engagement of missile formations, based on an analytic hierarchy process (AHP), and was used to calculate the fitness function. The proposed algorithm converges faster than the basic and adaptive PSO algorithms, and the optimal formation was acquired quickly and effectively.

In [24], the major factors affecting the defense deployment of air defense weapons against intelligent air strike weapons were analyzed. An adaptive PSO algorithm was proposed to compute the minimum kill path to air strike weapons, and was embedded in the fitness function of an outer PSO algorithm to form an adaptive nested PSO algorithm. The latter was used to obtain the optimal defense deployment of air defense weapons.

In this work, we use the basic PSO algorithm because its convergence performance is fair enough for our purpose. Due to imperfect kill probability, there is no steady-state optimal solution to converge to, even by applying other improved versions of PSO or machine learning algorithms. Considering the trade-off among computational load, convergence, and complexity, we used basic PSO in this work.

2.6. Defense Cost Function

The deployment of defense stations is optimized by minimizing a defense cost function, which is tailored to the prioritization of defense assets. In this work, four different types of defense cost function are specified:

$$\zeta_1 = N_{dt} + 0.5N_{dt'} + 0.2N_{ds} + 0.02N_{db} \quad \text{(benchmark)} \tag{11}$$

$$\zeta_2 = N_{dt} + 0.05N_{dt'} + 0.02N_{ds} + 0.002N_{db} \quad \text{(major post dominant)} \tag{12}$$

$$\zeta_3 = N_{dt} + N_{dt'} + 0.2N_{ds} + 0.02N_{db} \quad \text{(minor post on par with major post)} \tag{13}$$

$$\zeta_4 = N_{dt} + 0.5N_{dt'} + 0.5N_{ds} + 0.02N_{db} \quad \text{(defense station on par with minor post)} \tag{14}$$

where N_{dt} is the number of hits on the major post, $N_{dt'}$ is the number of hits on the minor posts, N_{ds} is the number of defense stations lost, and N_{db} is the number of interceptors consumed. The cost function ζ_1 can be used as a benchmark. One hit on the major post is arbitrarily allocated a relative cost of 1. Each minor post can serve as backup to the major post, thus 1 hit is allocated a relative cost of 0.5. A defense station is lost by taking 1 hit and is allocated a relative cost of 0.2. Each interceptor is allocated a relative cost of 0.02.

In cost function ζ_2, the importance of the major post is emphasized by reducing tenfold the cost of hit on minor posts and defense stations as well as the cost of interceptors, as compared to their counterparts in ζ_1. In cost function ζ_3, the importance of a minor post is promoted on par with the major post by imposing the same cost per hit. In cost function ζ_4, the importance of each defense station is promoted to match one hit on a minor post. The defense cost is counted at the end of each game for further statistical analysis.

2.7. Default Parameters in Simulations

Tables 1 and 2 list the parameters of the defense force and the attack force, respectively. The major post is located at (T_x, T_y), and the center of the deployment area shown in Figure 2. The particle position is confined by $x_{\max} = T_x + 50$, $x_{\min} = T_x - 50$, $y_{\max} = T_y + 200$ and $y_{\min} = T_y - 200$. Table 3 lists the parameters of optimization. The particle velocity is confined by $V_{x,\max} = 0.2(x_{\max} - x_{\min})$, $V_{x,\min} = -V_{x,\max}$, $V_{y,\max} = 0.2(y_{\max} - y_{\min})$ and $V_{y,\min} = -V_{y,\max}$.

A total of M defense stations are deployed to protect the assets from the attack force, and each defense station is armed with N_{br} interceptors. Each defense station is assigned a radius of coverage (R_r), within which any attacker can be marked for interception. The attacker impact radius (D_a) and interceptor impact radius (D_b) are effective ranges within which the attacker or interceptor will hit its target, with a given kill probability (p_k).

The radius of coverage (R_r), interceptor speed (v_b), attacker speed (v_a), interceptor impact radius (D_b), and attacker impact radius (D_a) are roughly estimated from available data collected from public sources. The maximum flight time of interceptor (B_τ) and

attacker (A_τ) are estimated from their respective maximum flight range. Empirically, neither interceptor nor attacker can guarantee to hit its intended target, and such uncertainty is characterized with a kill probability (p_k) derived from available records. When an aimed target falls within the impact radius of an interceptor or an attacker, the target will survive with probability of $1 - p_k$. The use of kill probability makes the game versatile and unpredictable, more or less reflecting the mist of wars.

Table 1. Parameters of defense force.

Parameter	Symbol	Value
major post coordinates	(T_x, T_y)	(381,250) km
minor post coordinates	-	(421,400) km, (421,100) km
number of defense stations	M	10
number of interceptors per defense station	N_{br}	8
radius of coverage	R_r	200 km
interceptor impact radius	D_b	50 m
interceptor speed	v_b	1 mach
interceptor flight time	B_τ	900 s
interceptor kill probability	p_k	0.7

Table 2. Parameters of attack force.

Parameter	Symbol	Value
number of attack stations	N_{sa}	10
number of attackers per attack station	N_{am}	4
departure angle	θ	30°
attacker impact radius	D_a	50 m
attacker speed	v_a	1 mach
attacker flight time	A_τ	1500 s
attacker alert radius	R_a	40 km
attacker maneuverability	α_e	0.5

Table 3. Parameters of optimization.

Parameter	Symbol	Value
time interval	Δt	20 s
number of particles	N	20
number of iterations	-	40
particle velocity weight	w_v	1
acceleration constants	(c_1, c_2)	(2, 2)

The total number of attack stations (N_{sa}) and the number of attackers (N_{am}) on each attack station determine the type and intensity of an assault mission, be it provocative, repressive, or fatal. The efficacy of N_{sa} and N_{am} also depends on the number of defense stations (M), the number of interceptors (N_{br}) on each defense station, and how these stations are deployed. Likewise, the efficacy of M and N_{br} depends on N_{sa}, N_{am}, the intention of attack force, and how much defense cost will be tolerated.

The deployment plan of defense stations is optimized under the worst condition that the attack force can achieve its best performance. The attack force puts the highest priority on the major post and the second priority on two minor posts. Thus, two diverse paths are planned from each attack station to the major post, one from left flank and the other from right flank. Both paths take off at a departure angle (θ) about a straight line between the major post and the attack station. Similarly, the path planned to attack a minor post or a defense station also takes off at departure angle θ.

An attacker is endowed certain self-defense capability. When an attacker finds itself being marked by an interceptor within alert radius (R_a), it will adjust its evading direction,

pending on its maneuverability (α_e). The attacker maneuverability increases its survivability, which in turn urges the defense force to optimize its deployment plan accordingly.

The simulation time interval (Δt) is fine enough to manifest the capability of all the agents based on the game rules, yet is coarse enough not to prolong the CPU time unnecessarily. In the PSO algorithm, the weight (w_v) and acceleration constants (c_1, c_2) on particle velocity are tuned to move the particles quickly to the global best position, without converging to local optimal positions. The number of particles (N), number of iterations, and particle velocity increment are fine-tuned by observing the convergence condition and the CPU time over many runs of simulation.

3. Simulation Results and Statistical Analysis

Given a formation of attack stations and a defense cost function chosen among Equations (11)–(14), the PSO algorithm is applied to search for a global best particle, which prescribes an optimal deployment plan of defense stations. Then, 100 games are played according to this deployment plan, and the resulting defense costs out of these games are sorted to derive a cumulative distribution function (CDF) for statistical analysis. In this section, the general statistical features on these 100 games will be reviewed and compared under two different attack formations and four different types of defense cost function. Some interesting outlier cases will be inspected in the next section to learn more about the nature of the game.

For each type of defense cost function, under slant or pincer attack formation, the PSO algorithm is applied four times, acquiring an optimal deploment plan each time. Each optimal deployment plan is then used to play 100 games and the resulting defense costs are presented in the form of a CDF curve. Figures 4 and 5 show the CDF curves on four types of defense cost function, against slant attack formation and pincer attack formation, respectively. For example, the four curves in Figure 4a are the results played with four optimal deployment plans, respectively, under cost function type of ζ_1, and their values lie in [1.7, 6.1], [2.8, 12], [2, 12.4] and [3.9, 9.6], respectively.

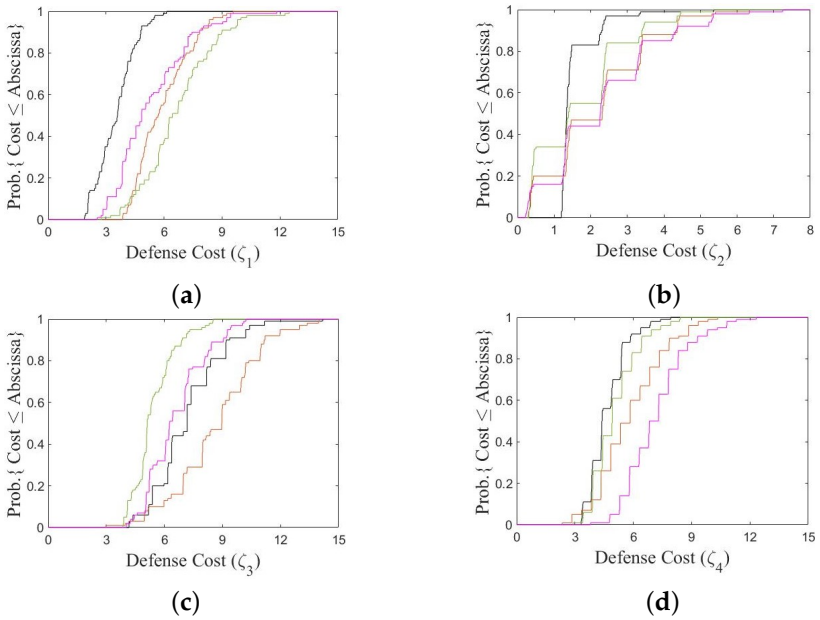

Figure 4. CDF of defense cost function against slant formation, (**a**) ζ_1; (**b**) ζ_2; (**c**) ζ_3; (**d**) ζ_4, with four PSO runs.

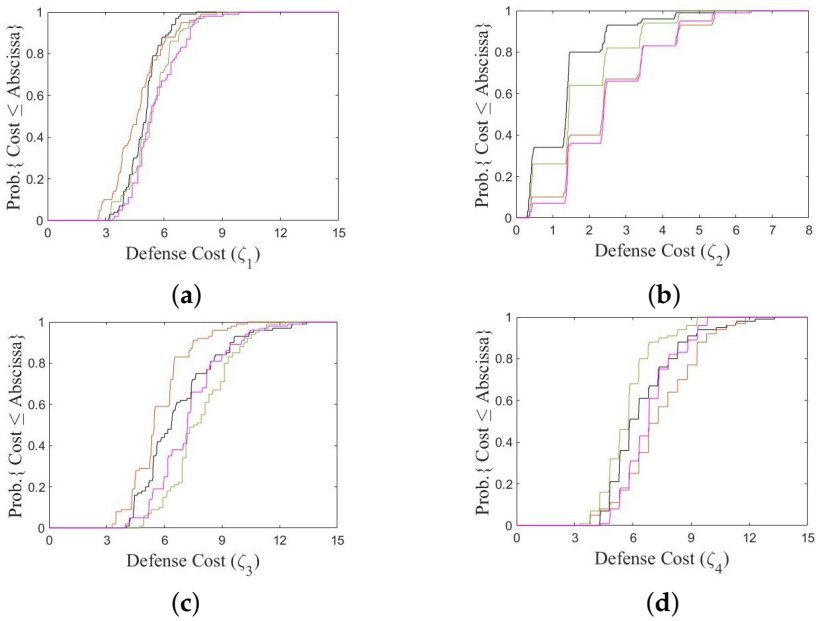

Figure 5. CDF of defense cost function against pincer formation, (**a**) ζ_1; (**b**) ζ_2; (**c**) ζ_3; (**d**) ζ_4, with four PSO runs.

One out of the four optimal deployment plans in Figure 4a that leads to the lowest median defense cost is selected to check how the defense cost of its associated global best particle converges with iterations. The black curve in Figure 6 shows such convergence with iterations for defense cost function of type ζ_1. Similarly, the other three curves in Figure 6 show the convergence of cost functions for types ζ_2, ζ_3, and ζ_4, associated with the curve with lowest median defense cost in Figures 4b–d, respectively.

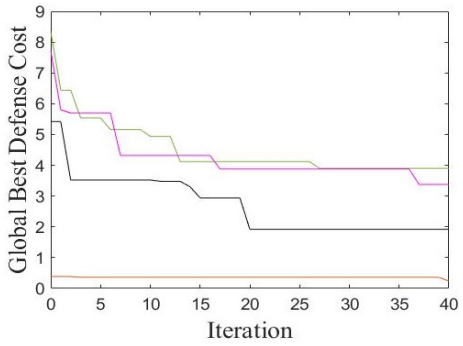

Figure 6. Convergence of defense cost against slant formation, black: ζ_1, orange: ζ_2, green: ζ_3, purple: ζ_4.

The convergent values of $\zeta_1, \zeta_2, \zeta_3$ and ζ_4 are 1.92, 0.24, 3.9, and 3.38, respectively. Due to the uncertainty aroused by imperfect kill probability, the defense cost may remain constant over many iterations before dropping to a lower value. The value of ζ_2 is relatively lower than the other three because the weighting on minor posts, defense stations and interceptors are reduced by tenfold compared with their counterparts in the benchmark case (ζ_1). On the other hand, the values of ζ_3 and ζ_4 are relatively higher due to the increased weighting on minor posts and defense stations, respectively. Similarly, Figure 7 shows the convergence of defense costs associated with four optimal deployment plans, one selected from each of the four subfigures in Figure 5, under pincer attack formation. The convergent values of $\zeta_1, \zeta_2, \zeta_3$ and ζ_4 are 2.72, 0.322, 4.24, and 4.26, respectively.

Figure 8a shows the optimal deployment plan of defense stations against slant attack formation, based on defense cost ζ_1. It is observed that three defense stations are placed within 40 km of the major post, and one defense station is placed within 40 km of the north and the south minor posts, respectively, Three defense stations are placed between the

major post and the south post to cover both, and three defense stations are placed in the upper left area to guard both the major post and the north post. More defense stations are placed within 40 km of the major post than within 40 km of the other two minor posts.

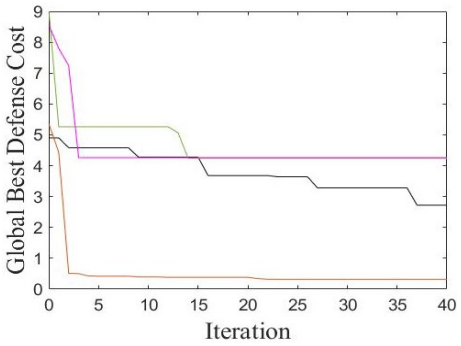

Figure 7. Convergence of defense cost against pincer formation, black: ζ_1, orange: ζ_2, green: ζ_3, purple: ζ_4.

Figure 8b shows the optimal deployment plan of defense stations based on defense cost ζ_2. It is observed that five defense stations are placed near the major post, with three of them within 40 km of the latter. Since the weighting on major post is highlighted, more stations are placed around it than on ζ_1. In addition, three defense stations are placed near the south post, with one within 40 km of the latter, two defense stations are placed west to guard the north post, but none of them are within 40 km of the north post. Compared to the deployment plan on ζ_1, the defense stations are clustered into several swarms or pairs, and the protection on minor posts becomes weaker since fewer defense stations are placed near them, due to the reduced weighting on minor posts.

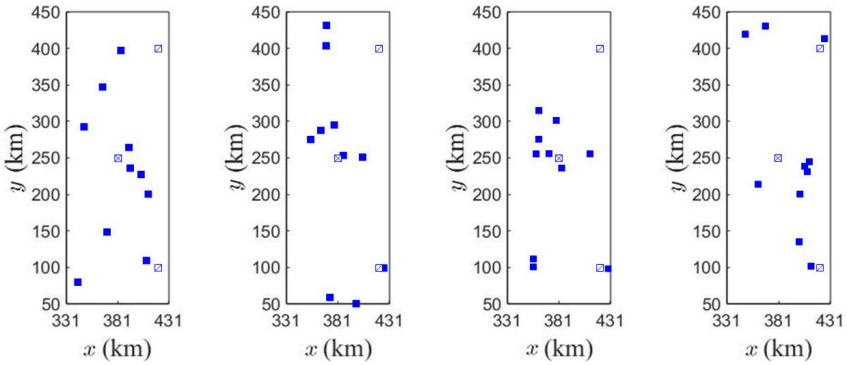

Figure 8. Optimal deployment of defense stations against slant formation, based on (**a**) ζ_1; (**b**) ζ_2; (**c**) ζ_3; (**d**) ζ_4, square with cross: major post, square with slash: minor post, blue square: defense station.

Figure 8c shows the optimal deployment plan of defense stations based on defense cost ζ_3. It is observed that most defense stations are placed near the major post, with five defense stations within 40 km of the latter. Two defense stations are placed far west to the south post to guard it, and one more defense station is placed close to the south post for reinforcement. However, no defense station is placed near the north post, and the nearest defense station is 103 km away. More defense stations are placed near the major post than near the south post although they have the same weighting because more attackers aim for the major post, which is closer to the attack stations than the south post.

Figure 8d shows the optimal deployment plan of defense stations based on defense cost ζ_4. It is observed that four defense stations are placed near the major post, with three defense stations within 40 km of the latter. Two defense stations are placed close to each other and west to the north post, and one more defense station is placed close to the north

post for reinforcement. Two defense stations are placed near the south post, with one within 40 km of the latter. In general, the defense stations are clustered near each protected post.

Figure 9a shows the optimal deployment plan of defense stations against pincer attack formation, based on defense cost ζ_1. It is observed that four defense stations are placed near the major post, with three of them within 40 km, to the east, southeast and south, respectively, of the major post. There are two defense stations near the north and the south posts, respectively, and each minor post has one defense station within 40 km. Since the major post has the highest weighting and is targeted by many more attackers, more defense stations are placed around it.

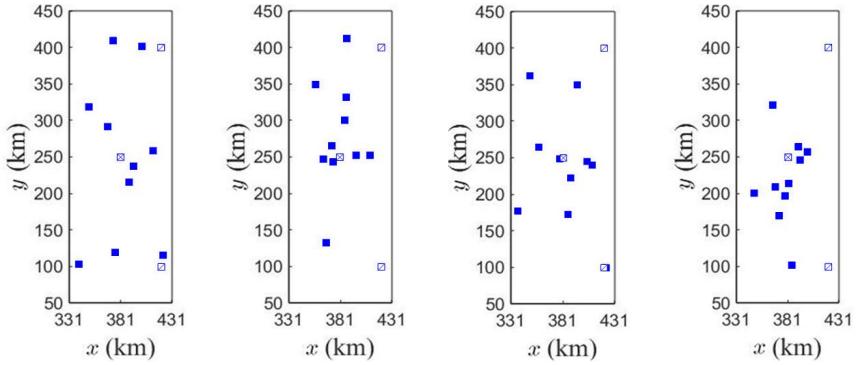

Figure 9. Optimal deployment of defense stations against pincer formation, based on (**a**) ζ_1; (**b**) ζ_2; (**c**) ζ_3; (**d**) ζ_4, square with cross: major post, square with slash: minor post, blue square: defense station.

Figure 9b shows the optimal deployment plan of defense stations based on defense cost ζ_2. Compare to that on ζ_1, more defense stations are placed near the major post because its relative weighting is highlighted. There are six defense stations near the major post, and five of them are within 40 km of the latter. One defense station is placed within 40 km to the north post, one defense station is placed near the south post, but is farther than 40 km away, and two defense stations are placed between the major post and the north post to cover both.

Figure 9c shows the optimal deployment plan of defense stations based on defense cost ζ_3. There are five defense stations within 40 km of the major post. The south post has one defense station within 40 km, but the north post has no defense station within 40 km. Although the weightings on major and minor posts are the same, more defense stations are placed around the major post because many more attackers target on it. There are two defense stations between the major post and the north post to cover both, and two defense stations between the major post and the south post to cover both.

Figure 9d shows the optimal deployment plan of defense stations based on defense cost ζ_4. There are six defense stations near the major post, four of them are within 40 km, with three to the east and one to the south. There is only one defense station to the west of the south post, within 40 km of the latter. However, it is surprising that no defense station is placed near the north post. Since the major post has the highest weighting and is targeted by many more attackers, more defense stations are placed around it. There is one defense station between the major post and the north post to guard both.

Table 4 lists the statistics of loss against slant attack formation, including average hits on the major post, north post and south post, respectively, the percentage of defense stations lost, interceptors launched, and attackers lost, respectively. The average defense cost, median of defense cost, 80%, and 95% confidence intervals (CIs) are also listed.

With the optimal deployment plan based on ζ_1, the average hits on the three posts are low since each post is guarded by at least one defense station within 40 km, and some defense stations are placed between two adjacent posts. The hits on the major post are higher than those on the two minor posts because many more attackers target at the former.

The hits on the south post (0.21) are lower than that on the north post (0.61). Both minor posts have a number of defense stations within 40 km, but there are more defense stations placed in the southern area (between south post and major post) than in the northern area (between north post and major post). One of the defense stations is hit by an attacker in the middle of the game, and an interceptor chasing this attacker is released to intercept another attacker aiming for the south post. In addition, another defense station attracts an assault to itself, relieving a possible hit on the south post. More interesting and enlightening details will be demonstrated in the next section.

Table 4. Statistics of loss against slant attack formation.

Defense Cost Function	ζ_1	ζ_2	ζ_3	ζ_4	Empirical
average hits on major post	0.73	1.35	0.13	0.77	1.57
average hits on north post	0.61	1.87	2.25	1.15	1.11
average hits on south post	0.21	0.66	0.72	0	0.33
defense stations lost (%)	43.3	30.2	40.1	36	56.1
interceptors launched (%)	81.925	81.738	81.613	86.388	82.513
attackers lost (%)	82.8	82.75	77.125	85.5	78.125
average defense cost	3.317	1.668	5.208	4.527	-
median of defense cost	3.3	1.34	5.1	4.39	-
80% confidence interval	2.1995	1.9986	2.2796	2.5582	-
95% confidence interval	3.579	3.0912	3.2401	3.0803	-

With the optimal deployment plan based on ζ_2, the average hit on the south post (0.66) is low, but that on the north post (1.87) is higher since no defense station is placed within 40 km of the latter. The hit on the major post (1.35) is the highest among all four cases. The loss rate of defense stations (30.2%) is lower than the other three cases because two out of four defense stations near the major post have some cohort defense stations within 40 km to cover them, One of these four stations is able to fire an additional interceptor upon an attacker within 50 km of of the former. It turns out that three of these stations are hard to kill, but the 4th one is hit for sure.

With the optimal deployment plan based on ζ_3, the average hit on the major post (0.13) is very low since many more defense stations are placed around it. On the other hand, the hit on the north post (2.25) is relatively high because no defense stations are placed nearby. The hit on the south post (0.72) is much lower than that on the north post because the former is guarded by two defense stations to the west and one defense station within 40 km of it. The attacker loss rate (77.125%) is the lowest among the four cases, which is related to the poor protection on the north post.

With the optimal deployment plan based on ζ_4, the average hit on the south post is 0, since each post is more evenly covered by defense stations, with at least one defense station within 40 km of it. The defense station loss rate (36%) is moderate compared with the other cases because the weighting of defense stations is raised to the level of a minor post.

The 80% confidence interval is the difference of defense costs at the 10th percentile and the 90th percentile of the CDF curve. Similarly, the 95% confidence interval is the difference of defense costs at the percentiles of 2.5 and 97.5 of the CDF curve. A small confidence interval implies a more predictable defense cost in any game, and a large confidence interval implies more uncertainty in the resulting defense cost.

Table 5 lists the statistics of loss against pincer attack formation. With the optimal deployment plan based on ζ_1, the average hit on the north post (0.09) is the lowest among all the four cases. The average hit on the south post (1.23) is higher than that on the north post, because the only defense station within 40 km of the former is placed on the flank instead of up front to guard off or attract the approaching attackers. Indeed, one of the

attackers aiming for the south post is almost certain to hit the latter. The average hit on the major post (1.81) is the highest among all the four cases, implying that three defense stations within 40 km of the major post are not enough for protection. The attacker loss rate (79.95%) is comparable to the other cases, which is related to the hits on the major post and the south post.

Table 5. Statistics of loss against pincer attack formation.

Defense Cost Function	ζ_1	ζ_2	ζ_3	ζ_4	Empirical
average hits on major post	1.81	0.93	1.03	0.9	2.67
average hits on north post	0.09	1.85	1.72	2.71	0.56
average hits on south post	1.23	1.8	0.33	0.77	1.24
defense stations lost (%)	48.3	29.2	55.7	41.8	54
interceptors launched (%)	82.9	84.113	80.488	80.75	90.763
attackers lost (%)	79.95	78.275	75.8	75.875	74.2
average defense cost	4.762	1.305	5.482	6.022	-
median of defense cost	4.6	1.344	5.33	5.8	-
80% confidence interval	3.618	2.1163	3.8185	3.5395	-
95% confidence interval	6.64	3.171	6.04	6	-

With the optimal deployment plan based on ζ_2, the average hit on the major post (0.93) is relatively low since five defense stations are placed within 40 km of the former. The average hit on the north post (1.85) is the highest among all the four cases. The only defense station within 40 km of the north post fires all the equipped interceptors, and the latter becomes a sitting duck for the attackers approaching later. The average hit on the south post (1.8) is the highest among all the four cases since no defense station is placed within 40 km of the south post. The only defense station placed between the south post and the south attack stations fires all the interceptors in the early stage, leaving the south post defenseless against the attackers approaching later. The defense stations loss rate (29.2%) is the lowest among all the four cases. The southernmost defense station is easily attacked since no other defense station is placed within 40 km of the former. All the other defense stations have some cohort stations within 40 km to cover them and are occasionally hit by detouring attackers originally aiming for another defense asset. The attacker loss rate (78.275%) is comparable to the other cases, which is related to the high hits on the north and south posts.

With the optimal deployment plan based on ζ_3, the average hit on the major post (1.03) is relatively low since five defense stations are placed within 40 km of the former. The average hit on the south post (0.33) is the lowest among all the four cases, because two attackers are hit by two interceptors fired from nearby defense stations, respectively, the interceptors originally chasing these two attackers are spared to pursue the other attackers aiming for the south post. The average hit on the north post (1.72) is moderate compared with the other cases while no defense station is placed within 40 km of the former. The defense station loss rate (55.7%) is the highest among all the four cases because two out of three defense stations that have no cohort station within 40 km of them and become easy targets when all their interceptors are exhausted. Some attackers originally aiming for the two hit defense stations detour to attack nearby defense stations. One of the nearby defense stations, without cover from other cohort stations within 40 km, already fired all its interceptors and becomes a sitting duck. The other nearby defense station still has some interceptors available, but one of the approaching attackers has already been marked by two interceptors. Abiding by the game rules, this defense station will not fire another interceptor against the approaching attacker, and is hit before the chasing interceptors can catch the latter. One defense station is almost guaranteed to be hit by an attacker, which originally aimed for the major post and

later detours to strike the former. The attacker loss rate (75.8%) is comparable to the other cases, which is related to the high hit number on the north post and the large number of lost defense stations.

With the optimal deployment plan based on ζ_4, the average hit on the major post (0.9) is the lowest among all the four cases since four defense stations are placed within 40 km of the former. The average hit on the south post (0.77) is relatively low, comparable to the low hit on the north post based on ζ_1, under slant attack formation. However, the average hit on the north post (2.71) is the highest among all the four cases since no defense station is placed around it. The attacker loss rate (75.875%) is comparable to other cases, which is related to the high hit number on the north post.

The 80% confidence interval lies between 2.1 and 3.9, and the 95% confidence interval lies between 3.1 and 6.7. Both values are higher than their counterparts under slant attack formation because the south attack stations are closer to the defense force, making the latter more difficult to protect.

Figure 10a shows that the CDF curves of impact score (hit) on the major post based on ζ_1 and ζ_4 are similar. The CDF curve on ζ_2 shows fewer games with score 0 but more games with score 1, compared with those on ζ_1 and ζ_4. The CDF on ζ_1 shows score 0 in 44 games, score 1 in 44 games, and the highest score is 3. The CDF on ζ_2 shows score 0 in 2 games, score 1 in 77 games, and the highest score is 5. The CDF on ζ_3 shows score 0 in 88 games and the highest score is 2. The CDF on ζ_4 shows score 0 in 39 games, score 1 in 46 games, and the highest score is 3. Since more defense stations are placed around the major post on ζ_3 as compared with ζ_1, ζ_2 and ζ_4, most games on ζ_3 result in lower score than on the other ζ's.

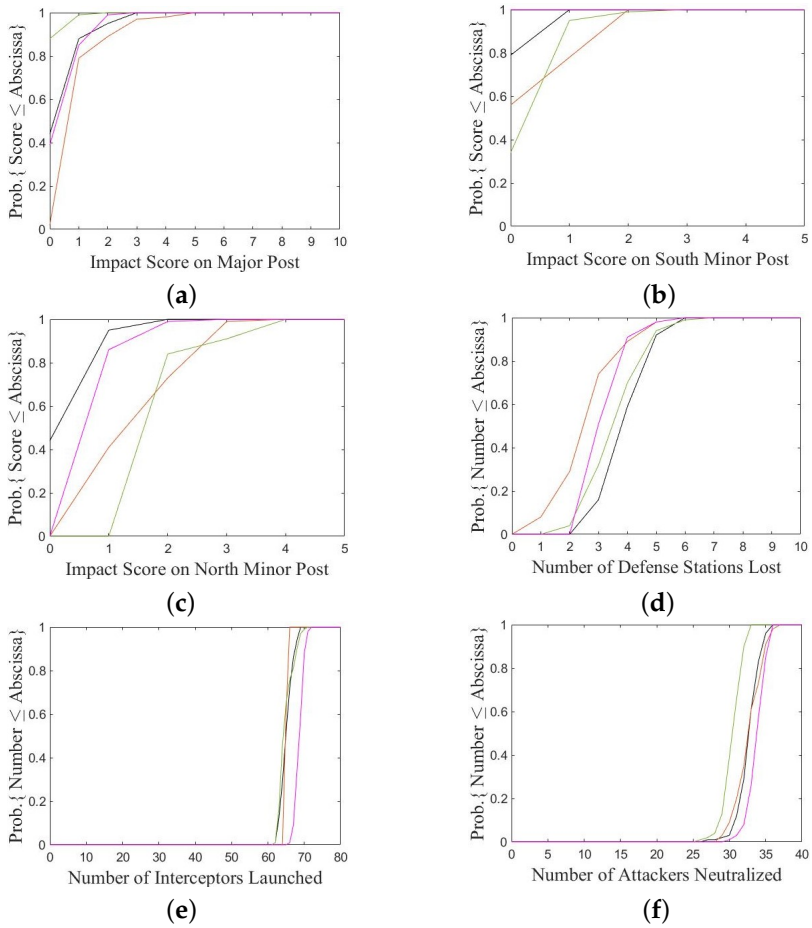

Figure 10. CDF of (**a**) impact score on major post; (**b**) impact score on south post; (**c**) impact score on north post; (**d**) number of lost defense stations; (**e**) number of launched interceptors; (**f**) number of lost attackers, against slant attack formation, black: ζ_1, orange: ζ_2, green: ζ_3, purple: ζ_4.

Figure 10b shows the CDF curves of impact score on the south post. In general, the scores on ζ_2 and ζ_3 are higher than those on ζ_1, which in turn are higher than those on ζ_4. The highest scores on ζ_1, ζ_2, ζ_3, and ζ_4 are 1, 2, 3, and 0, respectively. Score 0 is received in 79, 56, 34, and 100 games on ζ_1, ζ_2, ζ_3, and ζ_4, respectively.

Figure 10c shows the CDF curves of impact score on the north post. In general, the score is the highest on ζ_3, second on ζ_2, third on ζ_4 and the lowest on ζ_1. Based on ζ_1, ζ_2, ζ_3, and ζ_4, the lowest scores are 0, 1, 2, and 1, respectively, the highest scores are 2, 4, 4, and 3, respectively, and score 1 is received in 51, 41, 0, and 86 games, respectively. The highest score on the north post takes place on ζ_3 since no defense stations are placed around it. The scores on the north post on ζ_1 and ζ_4 are lower than that on ζ_2, since no defense stations are placed within 40 km of the north post on ζ_2.

Figure 10d shows that the least number of defense stations are lost on ζ_2 in most games, with 1 or 2 defense stations lost in 29 games. Based on ζ_1, ζ_2, ζ_3, and ζ_4, the lowest numbers of lost defense stations are 3, 1, 2, and 3, respectively, and the highest numbers of lost defense stations are 6, 6, 7, and 6, respectively.

Figure 10e shows that similar numbers of interceptors are fired on ζ_1, ζ_2 and ζ_3. The number ranges from 62 to 69 on ζ_1, from 65 to 66 on ζ_2, from 62 to 71 on ζ_3, and from 66 to 72 on ζ_4.

Figure 10f shows similar numbers of lost attackers on ζ_1 and ζ_2. Slightly more attackers are lost on ζ_4 in most games because all the posts are well protected, especially the south post. Fewer attackers are lost on ζ_3 in most games, which is related to the high score on the north post.

Figure 11a shows that the impact score on the major post is the highest on ζ_1, and similar on the other three ζ's. The higher score on ζ_1 in most games is related to the deployment of fewer defense stations within 40 km of the major post. Based on ζ_1, ζ_2, ζ_3, and ζ_4, the highest scores are 7, 4, 5, and 5, respectively, the score is 0 in 15, 38, 33, and 50 games, respectively, and the score is 1 in 33, 42, 41, and 24 games, respectively.

Figure 11b shows that the impact scores on the south post based on ζ_3 and ζ_4 are lower than the other two ζ's. The lower score on ζ_4 is attributed to the nearest defense station that not only intercepts some attackers but also attracts some attacker upon itself. The score on ζ_2 is the highest in most games because the nearest defense station is far away from the south post, and there is only one defense station between the south attack stations and the south post. Based on ζ_1, ζ_2, ζ_3, and ζ_4, the highest scores are 2, 3, 2, and 2, respectively, the score is 0 in 0, 0, 68, and 28 games, respectively, and the score is 2 in 23, 50, 1, and 5 games, respectively.

Figure 11c shows the CDF curves of impact score on the north post. The score on ζ_4 is the highest in most games because no defense station is placed nearby. The score on ζ_2 is slightly higher than that on ζ_3 in most games. The score on ζ_1 is the lowest in most games because two nearby defense stations are placed up front, attracting some attacker upon themselves. Based on ζ_1, ζ_2, ζ_3, and ζ_4, the highest scores are 1, 3, 4, and 5, respectively, and the lowest scores are 0, 1, 1, and 2, respectively. The score is 0 in 91 games on ζ_1, is 1 in 21 games and 2 in 73 games on ζ_2, is 1 in 39 games and 2 in 51 games on ζ_3, and is 2 in 48 games on ζ_4.

Figure 11d shows that the number of lost defense stations is the highest on ζ_3, second on ζ_1, third on ζ_4, and the lowest on ζ_2. Based on ζ_1, ζ_2, ζ_3, and ζ_4, the highest numbers are 6, 5, 7, and 7, respectively, and the lowest numbers are 4, 1, 5, and 2, respectively. The number of lost defense stations is 4 or 5 in 85 games on ζ_1, 2 or 3 in 61 games on ζ_2, 5 or 6 in 97 games on ζ_3, and 3 or 4 in 63 games on ζ_4.

Figure 11e shows that the number of launched interceptors is insensitive to the type of defense cost function. The CDF curves have steep slopes, which imply that a similar number of interceptors are fired in all the games. The number is 63 to 72 on ζ_1, 66 to 71 on ζ_2, 62 to 68 on ζ_3, and 63 to 68 on ζ_4.

Figure 11f shows that the number of lost attackers is similar in all four of the cases, which is 26 to 35 on ζ_1, 25 to 36 on ζ_2, 26 to 33 on ζ_3, and 25 to 34 on ζ_4. Slightly fewer attackers are lost when the attack stations are in pincer formation than in slant formation.

The simulations are run with MATLAB R2019a on a PC with i7-3.00GHz CPU and 32 GB memory. A typical game takes about 6.5–7.1 and 8.5–8.7 CPU hours when the attack stations are in slant and pincer formation, respectively, with kill probability of 0.7.

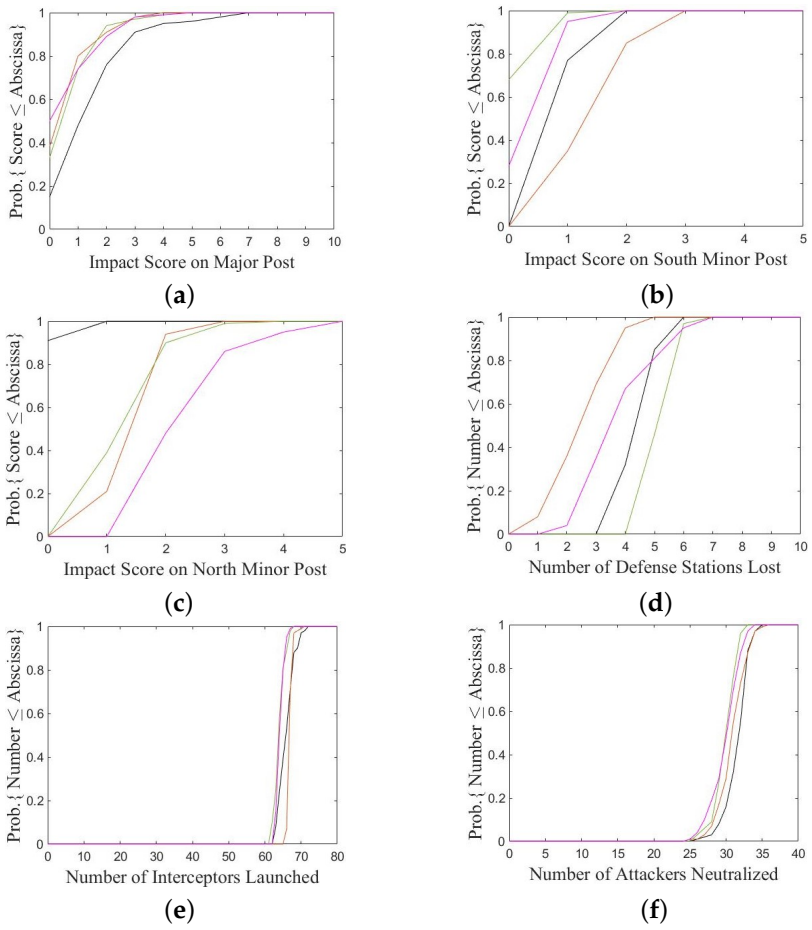

Figure 11. CDF of (**a**) impact score on major post; (**b**) impact score on south post; (**c**) impact score on north post; (**d**) number of lost defense stations; (**e**) number of launched interceptors; (**f**) number of lost attackers, against pincer attack formation, black: ζ_1, orange: ζ_2,green: ζ_3, purple: ζ_4.

4. Inspection of Some Interesting Outlier Cases

Given an attack formation and a type of defense cost function, the PSO algorithm is applied to acquire an optimal deployment plan of defense stations, which is used to play multiple games for statistical analysis. The imperfect kill probability of interceptors brings in uncertainty, and sometimes delivers unexpected results in terms of asset loss. In this section, four interesting outlier cases are inspected to learn more details about the game operations.

4.1. Case 1: On ζ_4 against Slant Formation, Low Score on South Post, and More Defense Stations Lost

In this case, an optimal deployment plan based on ζ_4 inflicts an unexpected low score on the south post but loses more defense stations than expected. By inspecting the game scenario, we find two defense stations near the south post attracting to themselves some attackers originally aiming for the south post, with each being pursued by more than two interceptors. Figure 12 shows some sequential footages in part of the deployment area to demonstrate the progress. The focus will be on the attackers originally assigned to the south post and the interceptors that pursue those attackers.

In the beginning, five attackers are assigned to strike the south post. One of the attackers is marked by two interceptors at an early stage and detours to strike the nearest defense station. Figure 12a shows that at $t = 860$ s, attackers A1, A2, A3, and A4 fly to the south post and are marked by interceptors B1, B2, B3, and B4, respectively. As A2, A3, and A4 manage to evade head-on hit, B2, B3, and B4 turn to tailgate A2, A3, and A4, respectively.

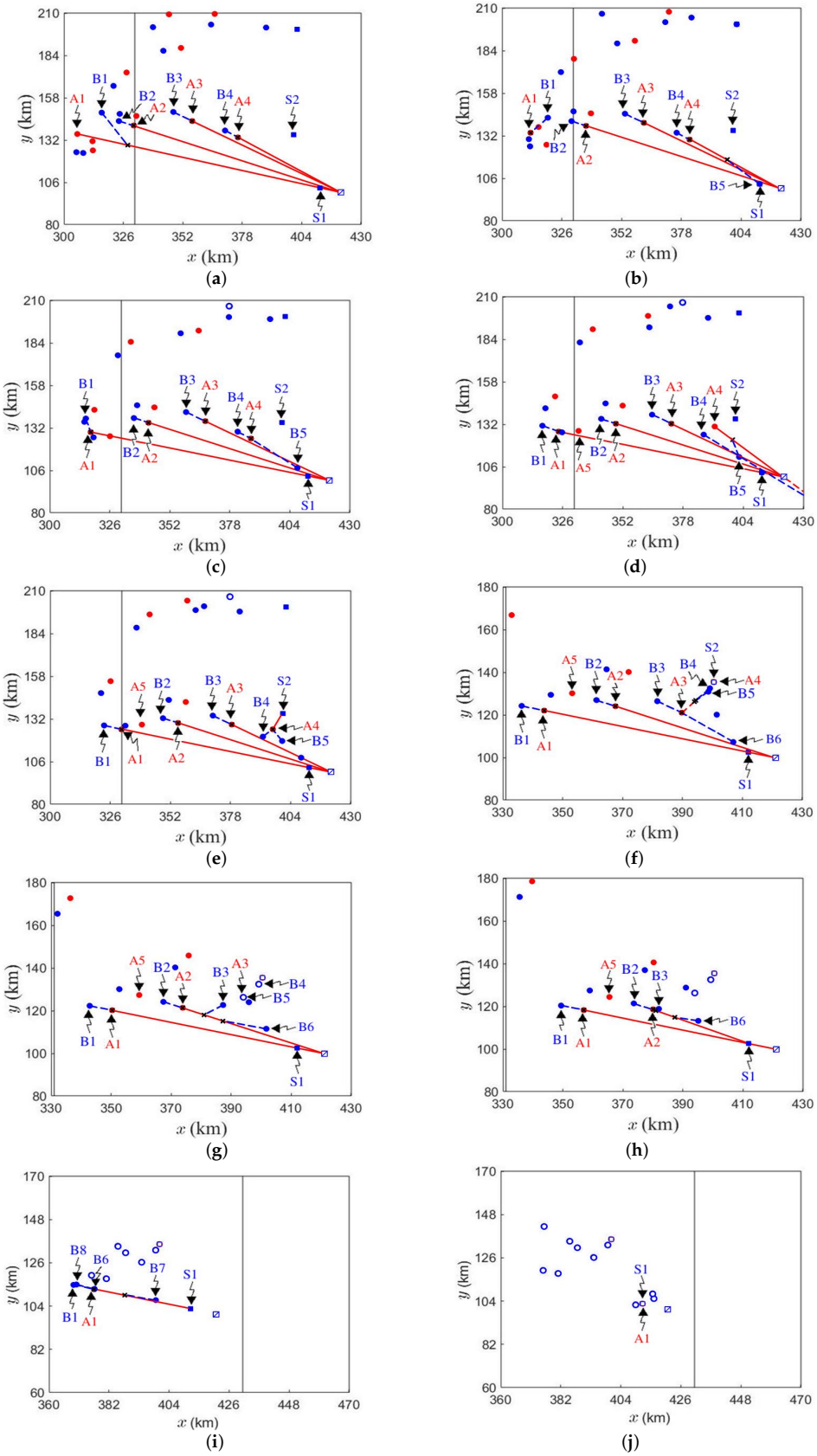

Figure 12. Scenario in case 1 on ζ_4, against slant formation, (**a**) $t = 860$ s; (**b**) $t = 880$ s; (**c**) $t = 900$ s; (**d**) $t = 920$ s; (**e**) $t = 940$ s; (**f**) $t = 980$ s; (**g**) $t = 1,000$ s; (**h**) $t = 1,020$ s; (**i**) $t = 1,080$ s; (**j**) $t = 1,240$ s, •: attacker, •: interceptor, square with cross: major post, square with slash: minor post, ———: planned attacker path, – – –: anticipated attacker path, – – –: anticipated interceptor path, ×: anticipated intercept point.

Figure 12b shows that, at $t = 880$ s, the nearest defense station S1 fires an interceptor B5 for A4 when the latter flies within 50 km of S1 and is marked by only one interceptor. Meanwhile, A1 finds itself marked by B1 and begins to turn its moving direction.

Figure 12c shows that at, $t = 900$ s, A4 finds itself marked by B5 and begins to turn its moving direction. Meanwhile, B1 loses the intercept point to A1 and turns to tailgate the latter.

Figure 12d shows that, at $t = 920$ s, A4 resumes its target after shaking off its chaser. Shortly after, interceptors B4 and B5 regain their intercept points, respectively, with A4.

Figure 12e shows that, at $t = 940$ s, A4 finds itself marked by two interceptors and changes its course to attack defense station S2, then B4 and B5 turn to tailgate A4. The scenario looks as if S2 attracts the assault of A4.

Figure 12f shows that, at $t = 980$ s, A3 makes turn to evade B6, then the latter changes its course to tailgate the former. Meanwhile, A4 hits S2 successfully, hence B4 and B5 are released to intercept the nearest attacker A3.

Figure 12g shows that, at $t = 1,000$ s, B4 burns out of fuel, A3 is hit by B5, hence B3 and B6 are released to intercept the nearest attacker A2.

Figure 12h shows that, at $t = 1,020$ s, A2 finds itself marked by more than one interceptor and detours to attack S1, as if S1 attracts the assault of A2. A2 is later hit by B3, releasing B2 to chase A5 and B6 for another nearby attacker.

Figure 12i shows that, at $t = 1,080$ s, B7 and B8 are chasing A1 after their previous target A5 was hit by B2. Meanwhile, B6 was released to hunt A1 after its previous target disappeared. B6 is 0.17 km from A1, A1 finds itself marked by two interceptors and detours to attack S1. Again, defense station S1 looks like it is attracting the assault of A1.

Figure 12j shows that, at $t = 1,240$ s, A1 manages to evade B1, B6, B7, and B8, then hits S1 successfully.

4.2. Case 2: On ζ_1 against Slant Formation, Low Score on North Post

In this case, an optimal deployment plan based on ζ_1 inflicts an unexpected low score on the north post. The nearest defense station to the north post is placed marginally within 40 km and west to the latter. If an attacker, marked by only one interceptor, flies within 50 km of the north post but farther than 40 km away, it will be hunted by an interceptor fired from this defense station. In addition, the defense station also attracts attackers to itself.

Figure 13 shows some sequential footages in part of the deployment area to demonstrate the progress of game. Figure 13a shows that, at $t = 580$ s, five attackers, A1, A2, A3, A4, and A5, are dispatched to attack the north post and are marked by interceptors B1, B2, B3, B4, and B5, respectively. Attacker A6 aims for the defense station closest to the north post and is marked by B6 and B7, and B7 is fired when A6 reaches within 50 km of the defense station. A4 and A5 are marked by additional interceptors B8 and B9, respectively, fired from the defense station closest to the north post as the former fly within 50 km but farther than 40 km of the latter.

Figure 13b shows that, at $t = 600$ s, A4 and A5 are hit by B8 and B9, respectively, then B4 and B5 detour to intercept A6. A6 is hit by B5 later, causing B4, B6, and B7 detour to hunt the nearest attacker A3.

Figure 13c shows that, at $t = 640$ s, A3 finds itself marked by more than one interceptor and detours to attack a defense station. An additional interceptor B10 hunts for A2 after the previous target of B10 disappeared. A3 is hit by B4 later, releasing B3, B6, and B7 to hunt for the nearest attacker A2.

Figure 13d shows that, at $t = 680$ s, A2 finds itself marked by more than one interceptor and detours to attack a defense station. A2 is hit by B3 later, releasing B2, B6, B7, and B10 to hunt for the nearest attacker A1.

Figure 13e shows that, at $t = 720$ s, A1 finds itself marked by more than one interceptor and detours to attack a defense station. A1 is hit by B10 at $t = 760$ s.

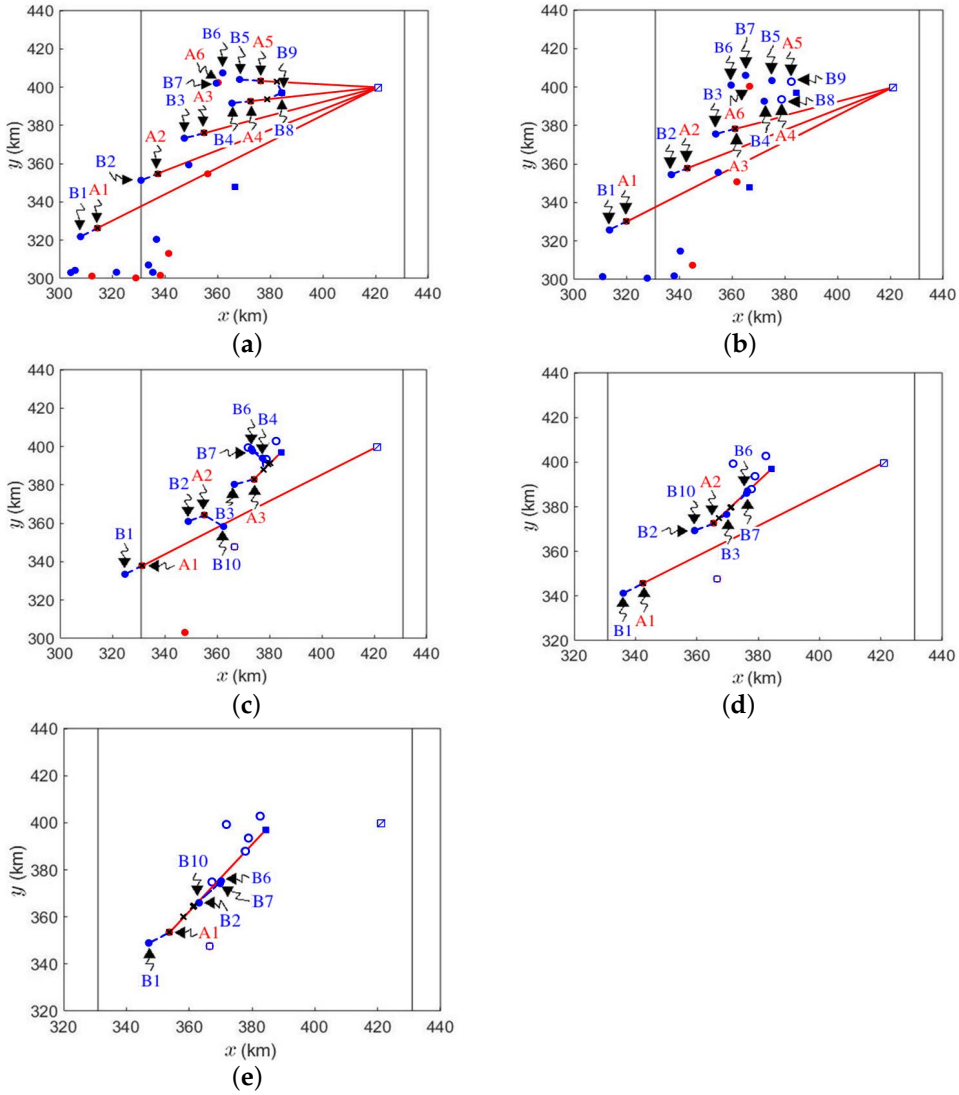

Figure 13. Scenario in case 2 on ζ_1, against slant formation, (**a**) $t = 580$ s; (**b**) $t = 600$ s; (**c**) $t = 640$ s; (**d**) $t = 680$ s; (**e**) $t = 720$ s.

4.3. Case 3: On ζ_2 against Slant Formation, High Score on Major Post

Table 4 shows that the average impact score on the major post based on ζ_2 is higher than those based on the other three types of defense cost function, regardless of five nearby defense stations. In this case, an attacker aiming for the major post finds at most one intercept point on its way to the major post, and is not marked by interceptors that detour from their previous targets. In addition, two defense stations supposed to intercept the attacker are not ready to fire along this attacker path.

Figure 14a shows that, at $t = 0$ s, Attacker A1, aiming for the major post, takes off and is immediately marked by interceptor B1 fired from the nearest defense station.

Figure 14b shows that, at $t = 40$ s, defense station S2 has fired all its interceptors, as enclosed in the circle.

Figure 14c shows that, at $t = 280$ s, A1 finds itself marked by B1 and turns its moving direction. Then, B1 loses the intercept point and turns to tailgate A1.

Figure 14d shows that, at $t = 300$ s, A1 resumes a straight path to strike the major post. B1 does not regain an intercept point and continues to tailgate A1.

Figure 14e shows that, at $t = 580$ s, B2 is fired from defense station S1 to intercept A1 since the latter flies within 50 km of its target. S2 has no spare interceptor against A1, and B1 continues to tailgate A1.

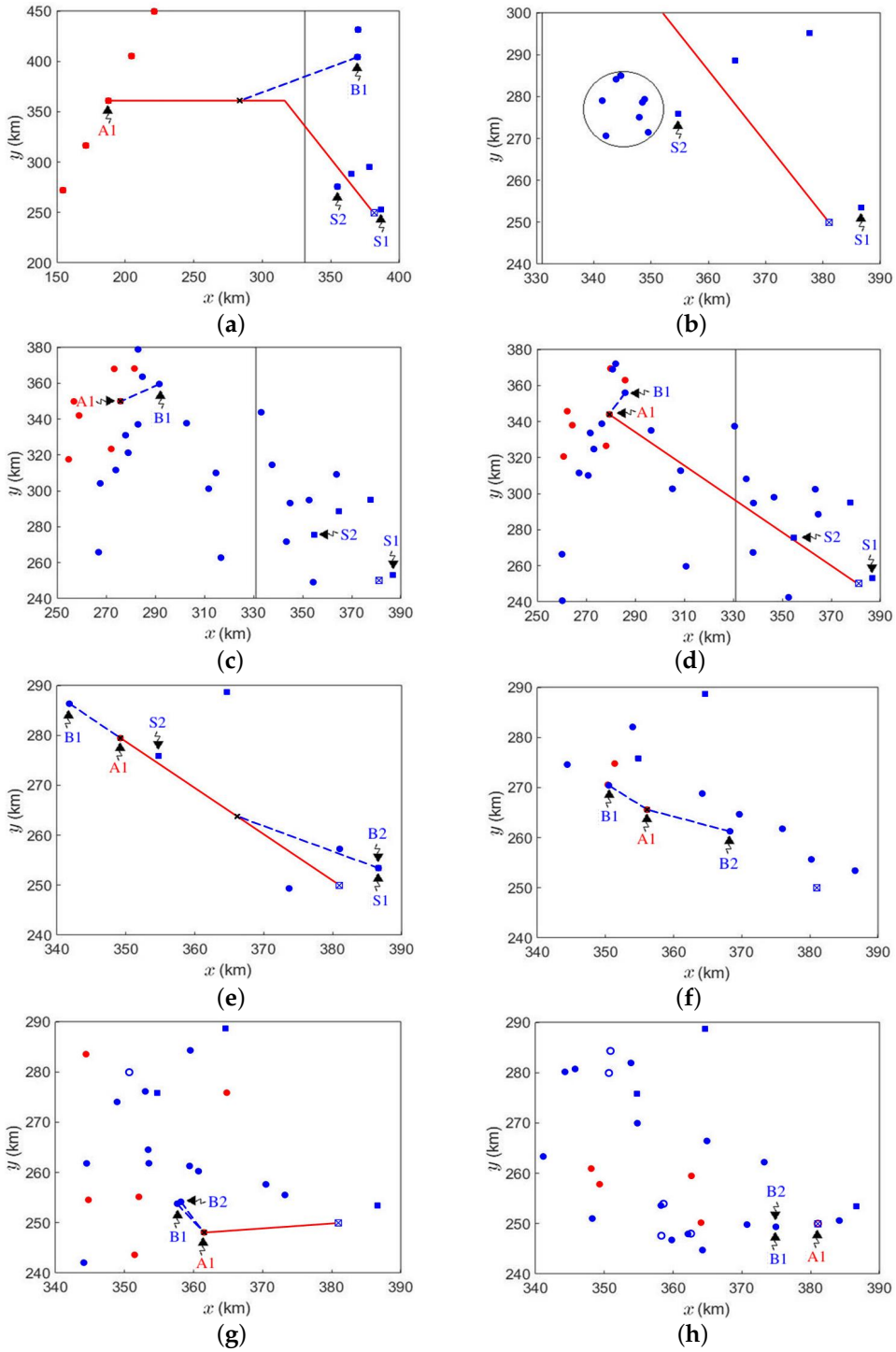

Figure 14. Scenario in case 3 on ζ_2, against slant formation, (**a**) $t = 0$ s; (**b**) $t = 40$ s; (**c**) $t = 280$ s; (**d**) $t = 300$ s; (**e**) $t = 580$ s; (**f**) $t = 640$ s; (**g**) $t = 700$ s; (**h**) $t = 760$ s.

Figure 14f shows that, at $t = 640$ s, A1 finds itself marked by B2 again and turns its moving direction. Then, B2 loses the intercept point again and turns to tailgate A1.

Figure 14g shows that, at $t = 700$ s, B2 continues to tailgate A1. A1 detects no intercept point and resumes a straight path to strike the major post.

Figure 14h shows that, at $t = 760$ s, A1 hits the major post.

4.4. Case 4: On ζ_1 against Pincer Formation, Low Score on North Post

In this case, an optimal deployment plan based on ζ_1 results in a very low impact score on the north post. An interceptor loses its target several times, then detours to hunt for another

nearby attacker, which in turn causes more attackers to strike the nearest defense station. The scenario appears as if two nearby defense stations attract some assaults to themselves.

Figure 15 shows a sequential footages around the north post. In the beginning, five attackers are dispatched for the north post, with one of them intercepted at an early stage. Figure 15a shows that, at $t = 540$ s, four attackers, A1, A2, A3, and A4, are marked by interceptors, B1, B2, B3, and B4, respectively. An attacker A5 aiming for defense station S2 is marked by interceptors B6 and B5, with the latter fired from S1 as A5 reaches within 50 km of its target.

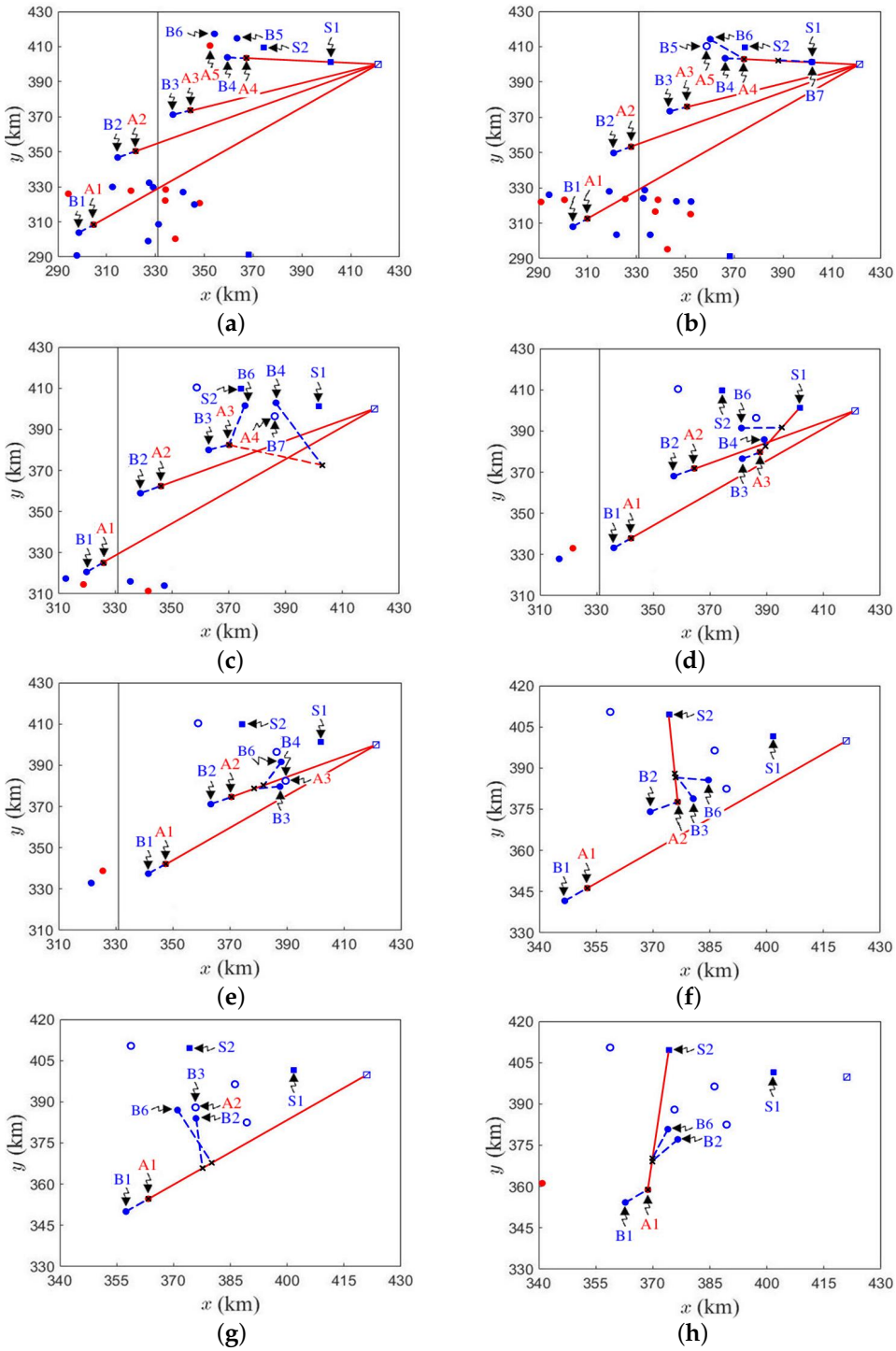

Figure 15. Scenario in case 4 on ζ_1, against pincer formation, (**a**) $t = 540$ s; (**b**) $t = 560$ s; (**c**) $t = 620$ s; (**d**) $t = 680$ s; (**e**) $t = 700$ s; (**f**) $t = 720$ s; (**g**) $t = 760$ s; (**h**) $t = 780$ s.

Figure 15b shows that, at $t = 560$ s, A5 is hit by B5, hence B6 takes its first detour to intercept A4. Meanwhile, an interceptor B7 is fired from defense station S1 to intercept A4 as the latter reaches within 50 km of its target.

Figure 15c shows that, at $t = 620$ s, A4 is hit by B7, releasing B4 and B6 to hunt A3. This is the second detour of B6. A3 finds itself marked by B6 and turns its moving direction.

Figure 15d shows that, at $t = 680$ s, A3 finds itself marked by B4 and B6, hence detours to attack the nearest defense station S1. Shortly after, B4 and B6 regain their intercept points, respectively, with A3.

Figure 15e shows that, at $t = 700$ s, A3 is hit by B4, releasing B3 and B6 to intercept the nearest attacker A2. This is the third detour of B6.

Figure 15f shows that, at $t = 720$ s, A2 finds itself marked by two interceptors, hence detours to attack the nearest defense station S2.

Figure 15g shows that, at $t = 760$ s, A2 is hit by B3, releasing B2 and B6 to intercept the nearest attacker A1. This is the fourth detour of B6.

Figure 15h shows that, at $t = 780$ s, A1 finds itself marked by two interceptors, hence detours to attack the nearest defense station S2. Finally, A1 is hit by B2 at $t = 820$ s.

5. Scenarios with Perfect Kill Probability

The imperfect kill probability of interceptors arouses uncertainty in every episode that an attacker falls within the impact radius of an interceptor. Hence, the outcomes of two games with the same attacker dispatch pattern and the same deployment plan of defense stations will not be the same. On the other hand, if the kill probability is set to 1, the outcome of a game will be predictable once the attacker dispatch pattern and the deployment plan of defense stations are specified. Theoretically, the PSO will converge to a steady-state global best position, based on the given type of defense cost function, which is then mapped to the optimal deployment plan.

Figure 16 shows the convergence of defense costs against slant attack formation. The convergent values of ζ_1, ζ_2, ζ_3, and ζ_4 are 2, 0.204, 1.74, and 2.24, respectively.

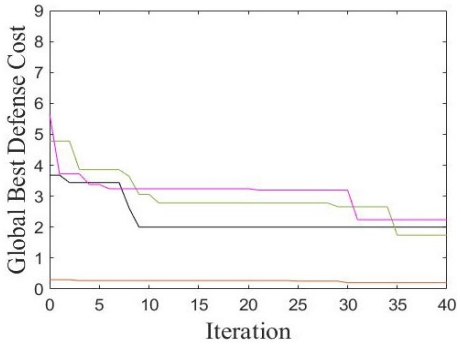

Figure 16. Convergence of defense cost against slant formation with kill probability set to 1, black: ζ_1, orange: ζ_2, green: ζ_3, purple: ζ_4.

Figure 17 shows the convergence of defense costs against pincer attack formation, all within 30 iterations. The convergent values of ζ_1, ζ_2, ζ_3, and ζ_4 are 2.5, 0.222, 3.4, and 2.4, respectively, which are higher than their counterparts against slant attack formation.

Figure 18a shows an optimal deployment plan of defense stations against slant attack formation, with kill probability set to 1, based on defense cost ζ_1. It is observed that two defense stations are placed within 40 km of the major post, four defense stations are placed near the north post, with 2 within 40 km of the latter, three defense stations are placed near the south post, with 1 within 40 km of the latter. The four defense stations around the north post are closer to the attack stations and will also intercept some attackers aiming for the major post.

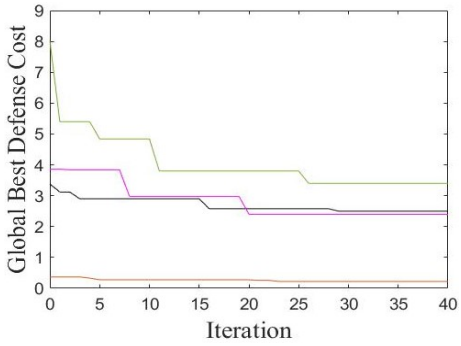

Figure 17. Convergence of defense cost against pincer formation with kill probability set to 1, black: ζ_1, orange: ζ_2, green: ζ_3, purple: ζ_4.

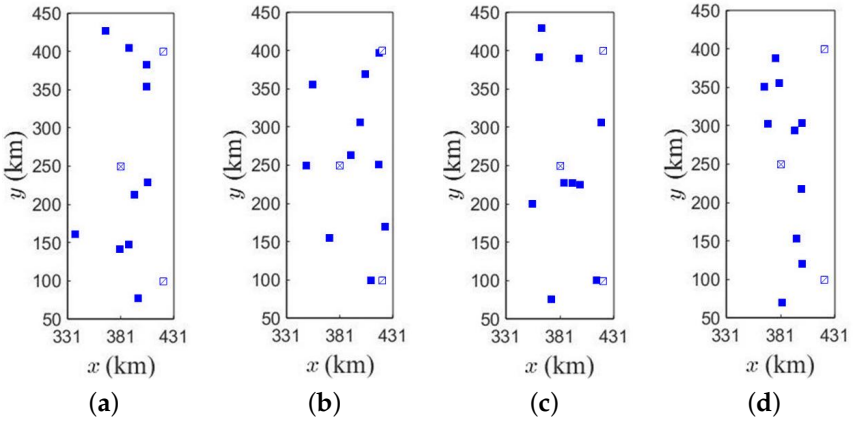

Figure 18. Optimal deployment plan of defense stations against slant attack formation, with kill probability set to 1, based on (**a**) ζ_1; (**b**) ζ_2; (**c**) ζ_3; (**d**) ζ_4; square with cross: major post, square with slash: minor post, blue square: defense station.

Figure 18b shows an optimal deployment plan of defense stations based on defense cost ζ_2. It is observed that three defense stations are placed within 40 km of the major post, more than that on ζ_1, possibly because the weighting of one hit on the major post is relatively higher. Two defense stations are placed southwest to the north post within 40 km of the latter, and one defense station is placed west to the south post within 40 km of the latter, two defense stations are placed between the major post and the north post to cover both, and two defense stations are placed between the major post and the south post to cover both.

Figure 18c shows an optimal deployment plan of defense stations based on defense cost ζ_3. There are four defense stations placed near the major post, with three within 40 km of the latter, three defense stations are placed near the north post, with one within 40 km of the latter, two defense stations are placed near the south post, with one to the west and within 40 km of the latter. The major post is covered by more defense stations within 40 km of the former since it is targeted by many more attackers. The south post is the farthest from the attack stations, hence is covered with fewer defense stations.

Figure 18d shows an optimal deployment plan of defense stations based on defense cost ζ_4. There are four defense stations placed near the major post, with one to the southeast within 40 km of the latter, three defense stations are placed near the north post, but none is within 40 km of the latter, and three defense stations are placed near the south post, with one to the northwest and within 40 km of the latter. Compared to the other three types of defense cost function, only the north post under ζ_4 has no defense station within 40 km of it, possibly because the weighting on each defense station is on par with one hit on the north post.

Figure 19a shows an optimal deployment plan of defense stations against pincer attack formation, with kill probability set to 1, based on defense cost ζ_1. There are six defense

stations placed within 40 km of the major post, one defense station is within 40 km of the north post, and two defense stations are near the south post, but not within 40 km of the latter. One defense station is placed between the major post and the north post to cover both. More defense stations are placed around the major post as compared to the counterpart case under slant attack formation, because the south attack stations are closer to the major post now.

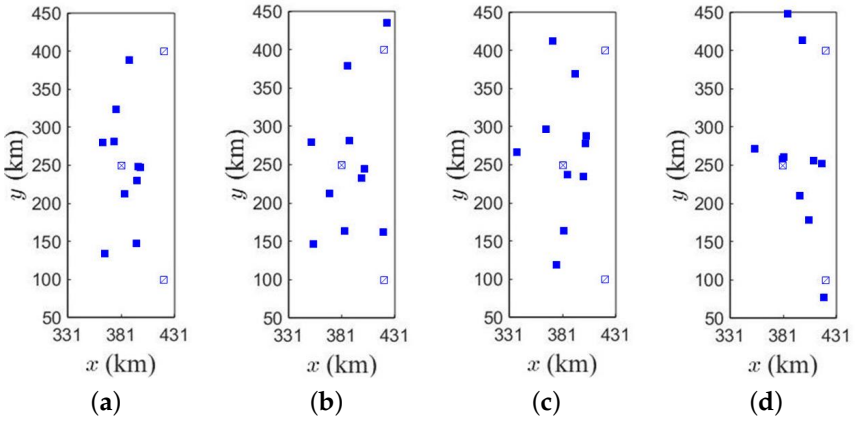

Figure 19. Optimal deployment plan of defense stations against pincer attack formation, with kill probability set to 1, based on (**a**) ζ_1; (**b**) ζ_2; (**c**) ζ_3; (**d**) ζ_4, square with cross: major post, square with slash: minor post, blue square: defense station.

Figure 19b shows an optimal deployment plan of defense stations based on defense cost ζ_2. There are five defense stations placed near the major post, with four within 40 km of the latter, two defense stations are placed near the north post, with one to the north and within 40 km of the latter. No defense station is placed within 40 km of the south post, three defense stations are placed between the major post and the south post to cover both. The number of defense stations near the major post is compatible with the case on ζ_1.

Figure 19c shows an optimal deployment plan of defense stations based on defense cost ζ_3. There are six defense stations placed near the major post, with three within 40 km of the latter, two and one defense stations are placed near the north post and the south post, respectively, but none of them are within 40 km of either post, and one defense station is placed between the major post and the south post to cover both. Although the weighting of a minor post is on par with the major post, the major post is still covered with many more defense stations because it is targeted by many more attackers than a minor post.

Figure 19d shows an optimal deployment plan of defense stations based on defense cost ζ_4. There are six defense stations placed near the major post, with five within 40 km of the latter, two defense stations are placed near the north post, with one within 40 km of the latter, one defense station is placed to the south of the south post and within 40 km of the latter, and one defense station is placed between the major post and the south post to cover both.

As was mentioned in the beginning of this section, the deployment plan of defense stations determines the script and outcome of any game if the kill probability is set to 1. With the deployment plans shown in Figure 18, the impact score on the major post is 0 on all the four types of defense cost function. The scores on the south post are 0, 0, 0, and 1 on ζ_1, ζ_2, ζ_3, and ζ_4, respectively. The score of 1 on ζ_4 is made by one attacker which successfully evades two interceptors, with one of them fired from a defense station within 40 km of the south post. The attacker finds at most one intercept point on route. The scores on the north post are 1, 0, 0, and 1 on ζ_1, ζ_2, ζ_3, and ζ_4, respectively. The score of 1 on ζ_4 is taken because no defense station is placed within 40 km of the north post. In spite of four defense stations around and 2 within 40 km of the north post, the score of 1 on ζ_1 is taken by one attacker which successfully evades two interceptors, one of them is fired from a

defense station south to and within 40 km of the north post. The attacker finds at most one intercept point on route.

There are 1, 4, 2, and 0 defense stations lost on ζ_1, ζ_2, ζ_3, and ζ_4, respectively. The high loss number on ζ_2 includes three defense stations which fire all the interceptors and no other defense stations are within 40 km to cover them. There is no loss on ζ_4 because the weighting of a defense station is on par with a minor post and the defense stations are well deployed to cover one another. Based on ζ_1, ζ_2, ζ_3, and ζ_4, the numbers of interceptors fired are 65, 62, 67, and 62, respectively, and the numbers of lost attackers are 38, 36, 38, and 38, respectively, both are insensitive to the type of defense cost function.

In case the attack stations are in pincer formation, the impact score on the major post is 0 on all four of the types of defense cost function. Note the number of defense stations around the major post is many more than that under attack in slant formation, as the south attack stations are closer to the major post. The score on the south post is 1 in all four of the types. On ζ_1, ζ_2, and ζ_3, there is no defense station placed within 40 km of the south post. On ζ_4, the only defense station near the south post fires six interceptors in the early stage, and the remaining two interceptors are not enough to guard off the attackers flying within 50 km of the south post later.

The scores on the north post are 1, 0, 0, and 1 on ζ_1, ζ_2, ζ_3, and ζ_4, respectively. On ζ_1, the only defense station near the north post fires all the interceptors in the early stage, leaving none against the attackers flying within 50 km of the north post later. On ζ_2, one defense station is placed within 40 km of the north post, and the other nearby defense station attracts some assaults to itself. The reason of score 0 on ζ_3 is more intricate. One attacker originally aiming for the north post finds itself marked by two interceptors, hence detours to attack the northernmost defense station together with another attacker. Then, the interceptors originally targeting at these two attackers detour to intercept other follow-up attackers, hitting them or forcing them to attack another defense station. The score on ζ_4 is made by one attacker which successfully evades two interceptors, with one of them fired from the nearest defense station within 40 km of the north post. The attacker finds at most one intercept point on route.

The defense stations lost on ζ_1, ζ_2, ζ_3, and ζ_4 are 1, 2, 6, and 0, respectively. On ζ_3, three defense stations fire all the interceptors in the early stage and have no other defense station within 40 km to cover them. Later on, some interceptors lose their marked attackers and detour to hunt for another attacker, forcing the latter to detour for the nearest defense station. Some attackers, with their target defense station destroyed, detour to strike another defense station. In addition, one attacker aiming for the major post detours for a defense station when it finds itself marked by two interceptors, with one fired from a defense station within 40 km of the major post. There is no defense station lost on ζ_4 because the weighting of a defense station is on par with a minor post.

The numbers of interceptors fired on ζ_1, ζ_2, ζ_3, and ζ_4 are 65, 66, 60, and 70, respectively. The number on ζ_3 is the lowest since only three defense stations are placed within 40 km of any post, hence fewer attackers are detected within 50 km of their targets to trigger interceptor firing. The number on ζ_4 is the highest since seven defense stations are placed within 40 km of any post, hence more attackers are detected within 50 km of their targets to trigger interceptor firing.

The numbers of lost attackers on ζ_1, ζ_2, ζ_3, and ζ_4 are 37, 37, 32, and 38, respectively. The relatively high numbers on ζ_1, ζ_2, and ζ_4 are related to the relatively low number of lost defense stations. On the other hand, the low number on ζ_3 is related to the high number of lost defense stations.

6. Comparisons and Discussion

Figure 3 shows that the attacker loss rate is about 58%, with attacker maneuverability of 0.5 and kill probability of 0.7. Table 4 shows that the attacker loss rate is raised to the level of 80% on any type of defense cost function, which implies the deployment plan of defense stations indeed takes significant effect.

Next, compare the deployment plans (kill probability of 0.7) in Figures 8 and 9 with their counterparts (kill probability of 1) in Figures 18 and 19, respectively. It is observed that the defense stations are deployed more dispersedly if the kill probability is 1, which implies that fewer defense stations are required to protect the major post. In contrast, it is more difficult to protect the assets if the kill probability is reduced to 0.7 because some attackers may survive the interceptors and strike the defense assets. However, an optimal deployment plan of defense stations does raise the level of protection on all the assets, with kill probability of 0.7, which is verified by comparing the loss rate of attackers in Figure 3 with those in Tables 4 and 5.

By comparing the data in Table 4 under slant formation and Table 5 under pincer formation, it is found that the impact scores on the major post and the south post are generally higher under pincer formation, especially the south post, since the southern attack stations are closer to both posts.

By comparing the deployment plans in Figures 18 and 19, it is observed that more defense stations are clustered near the major post than near the south post under pincer formation. The attack force under pincer formation imposes the same level of threat from north and south to the defense force, and the two forces are closer than under slant formation, hence the defense stations are pushed to cluster near the major post.

In contrast, the deployment plans in Figures 8 and 9 show that the number of defense stations near the major post does not increase under pincer formation on ζ_1 or ζ_3. With kill probability of 0.7, some attackers will survive the interceptors and strike the major post under either attack formation, and merely increasing the number of defense stations does not prevent this from happening.

It is observed that deploying more defense stations within 40 km of an asset offers better protection. Take for example, the protection of major post on ζ_3 under slant formation and on ζ_2, ζ_3, and ζ_4 under pincer formation, all with kill probability of 0.7. Nearby defense stations can attract some assaults to themselves and fire additional interceptor upon an attacker if the latter is marked by only one interceptor.

Deploying enough defense stations around an asset is crucial, placing them at right spots also matters. Take, for example, the protection of major post on ζ_2 under slant formation, with kill probability of 0.7 and the protection of north post on ζ_1 under slant formation, with kill probability of 1, are compromised because some attackers maneuver to break through the defense stations.

At a first glance, placing a defense station within 40 km of the protected asset can impede the attackers by firing additional interceptors or attracting some assaults to itself. However, attackers can sometimes survive interceptors even with some defense stations placed within 40 km of the asset. There are many episodes that an attacker is almost certain to hit its target which is covered by some defense stations within 40 km of the target. Two examples are the major post on ζ_2 under slant formation and the south post on ζ_1 under pincer formation, both with kill probability of 0.7. Additional examples include the south post on ζ_4 under slant formation, the north post on ζ_1 under slant formation and the north post on ζ_4 under pincer formation, all with kill probability of 1.

In general, placing defense stations at proper sites within 40 km of the protected asset is effective for intercepting approaching attackers. A rule of thumb is to place a defense station on a line between the protected asset and an approaching attacker, close to and shorter than 40 km from the asset. Take, for example, the protection of north post on ζ_1 under slant formation and the south post on ζ_4 under pincer formation, both with kill probability of 0.7. Another rule of thumb is to place a defense station very closely behind the protected asset. Take, for example, the protection of south post on ζ_3 under pincer formation, with kill probability of 0.7.

It is observed that, when an attacker hits its target or gets hit, the remaining interceptors in the pursuit are likely to detour against the follow-up attackers flying in the proximity. Hence, the north or south post can be well protected by placing only one defense station within 40 km of the asset, at the position that favors the interception of the first one or two

approaching attackers, then the follow-up attackers will be easier to hit. Take, for example, the protection of north post on ζ_1 under slant formation, with kill probability of 0.7, as well as the north post on ζ_1, the south post on ζ_3 and ζ_4, all under pincer formation, with kill probability of 0.7.

In summary, to better protect an asset, it is suggested to place a defense station on a line between the protected asset and approaching attacker, close to but shorter than 40 km from the asset. Another suggestion is to place a defense station very closely behind the protected asset to hit the approaching attackers, or place some nearby defense stations west, northwest or southwest to the protected asset to attract some assaults. More defense stations should be deployed close to the protected asset if more attackers are expected.

Comparing the average hits on posts with imperfect kill probability in Table 4 and Table 5 to the hits on posts with perfect kill probability, it appears more difficult to defend the assets with imperfect kill probability.

Note that the game design and the simulation results in this work are limited to aerial war games in 2D space, and the attackers and interceptors can only fly at constant speeds.

7. Empirical Deployment Plans

Based on the empirical rules of thumb learned from the simulations, as summarized in the last section, as well as intuitive observations on the deployment plans shown in Figures 8 and 9, we manually draw the empirical deployment plans of defense stations in Figure 20a,b against slant attack formation and pincer attack formation, respectively. The goal of these deployment plans is to protect all the three posts at the same priority, without resorting to specific type of defense cost function. The efficacy of these deployment plans is tested with the kill probability of 0.7.

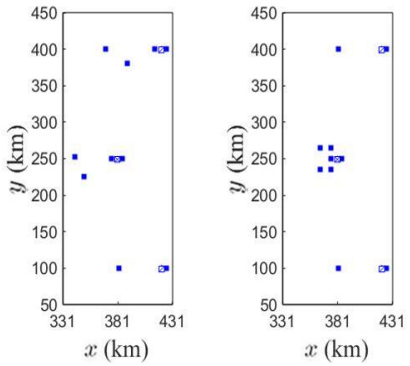

Figure 20. Empirical deployment plan of defense stations against (**a**) slant attack formation and (**b**) pincer attack formation, with kill probability of 0.7, square with cross: major post, square with slash: minor post, blue square: defense station.

Figure 20a shows the empirical deployment against slant attack formation, in which 4, 4, and 2 defense stations are placed near the major post, north minor post and south minor post, respectively. Among these defense stations, 4, 3, and 2 of them are placed within 40 km of the major post, north minor post, and south minor post, respectively. Fewer defense stations are placed around the south post because it is farther away from the attack stations and is targeted by fewer attackers than the major post. A defense station is put slightly behind each post, and a defense station is put slightly in front of the major post and the north post, respectively, to attract some assaults. A defense station is put southwest to the major post to also cover the south post.

The statistics of loss based on the empirical deployment plan against slant attack formation are also listed in Table 4. The average hits on the major post (1.57) is higher than all the other four deployment plans. The average hits on the north minor post is higher than that on ζ_1, close to that on ζ_4, and lower than that on ζ_2 or ζ_3. The average hits on the

south minor post is higher than that on ζ_1 or ζ_4, but lower than that on ζ_2 or ζ_3. The defense stations lost (56.1%) is higher than all the other four deployment plans. The attackers lost (78.125%) is close to that on ζ_3, and lower than those on the other three deployment plans. These numbers suggest that the optimal deployment plan based on either type of defense cost function is generally more effective in protecting the major post, inflicting fewer loss of defense stations and more loss of attackers.

Figure 20b shows the empirical deployment against pincer attack formation, in which 6, 2, and 2 defense stations are placed near the major post, north minor post, and south minor post, respectively. All the defense stations are placed within 40 km of a post. Due to the symmetry of pincer attack formation, the defense stations are deployed symmetrically in the north-south direction. Compared with Figure 20a, more defense stations are placed near the major post because the southern attack stations are closer to the major post in Figure 20b. A defense station is put slightly behind each post, five defense stations are put in front of the major post to attract some assaults, and a defense station is put at 40 km to the west of the north post and the south post, respectively. The two defense stations farthest from the major post launch interceptors in the early stage, and the other defense stations near the major post are reserved to intercept the attackers in the later stage.

The statistics of loss based on the empirical deployment plan against pincer attack formation are also listed in Table 5. The average hits on the major post (2.67) is higher than all the other four deployment plans. Compared to the case under slant attack formation, the average hits is higher since the southern attack stations are closer to the major post. The average hits on the north minor post (0.56) is higher than that on ζ_1 but is lower than that on ζ_2, ζ_3, or ζ_4. The average hits on the south minor post (1.24) is close to that on ζ_1, lower than that on ζ_2, and higher than that on ζ_3 or ζ_4. The defense stations lost (54%) are close to that on ζ_3, but is higher than that on ζ_1, ζ_2, or ζ_4. The interceptor launched (90.763%) is higher than all four of the other deployment plans, perhaps because all the defense stations are placed within 40 km of their protected post. The attackers lost (74.2%) is close to that on ζ_3 or ζ_4, but lower than that on ζ_1 or ζ_2.

Figure 21a shows the CDF of impact score on the major post. The impact score under pincer attack formation is statistically higher than that under slant attack formation. Out of 100 games, 91 have scores lower than 4 under slant formation, and 70 have score lower than 4 under pincer formation. The maximum and minimum possible scores under both attack formations are 6 and 0, respectively.

Figure 21b shows the CDF of impact score on the south post. The impact score under pincer formation is statistically higher than that under slant formation. Out of 100 games, 70 have zero score under slant formation, and 79 have score 1 under pincer formation. The maximum and minimum possible scores under slant formation are 2 and 0, respectively, and the maximum and minimum possible scores under pincer formation are 3 and 1, respectively.

Figure 21c shows the CDF of impact score on the north post. The impact score under slant formation is statistically higher than that under pincer formation. Out of 100 games, 78 have score 1 under slant formation and 58 have zero score under pincer formation. The maximum and minimum possible scores under both attack formations are 2 and 0, respectively.

Figure 21d shows the CDF of lost defense stations. The number of defense stations lost are statistically similar under both formations. Out of 100 games, 82 have 5 or 6 lost defense stations under slant formation, and 81 have 4–6 lost defense stations under pincer formation. The maximum and minimum possible numbers under slant formation are 7 and 4, respectively, and the maximum and minimum possible numbers under pincer formation are 8 and 4, respectively.

Figure 21e shows the CDF of interceptors launched. The numbers under pincer formation are statistically higher than those under slant formation. The maximum and minimum possible numbers under slant formation are 68 and 64, respectively, and the maximum and minimum possible numbers under pincer formation are 75 and 71, respectively.

Figure 21f shows the CDF of lost attackers. The numbers under slant formation are statistically higher than those under pincer formation. The maximum and minimum possible numbers under slant formation are 35 and 25, respectively, and the maximum and minimum possible numbers under pincer formation are 35 and 22, respectively.

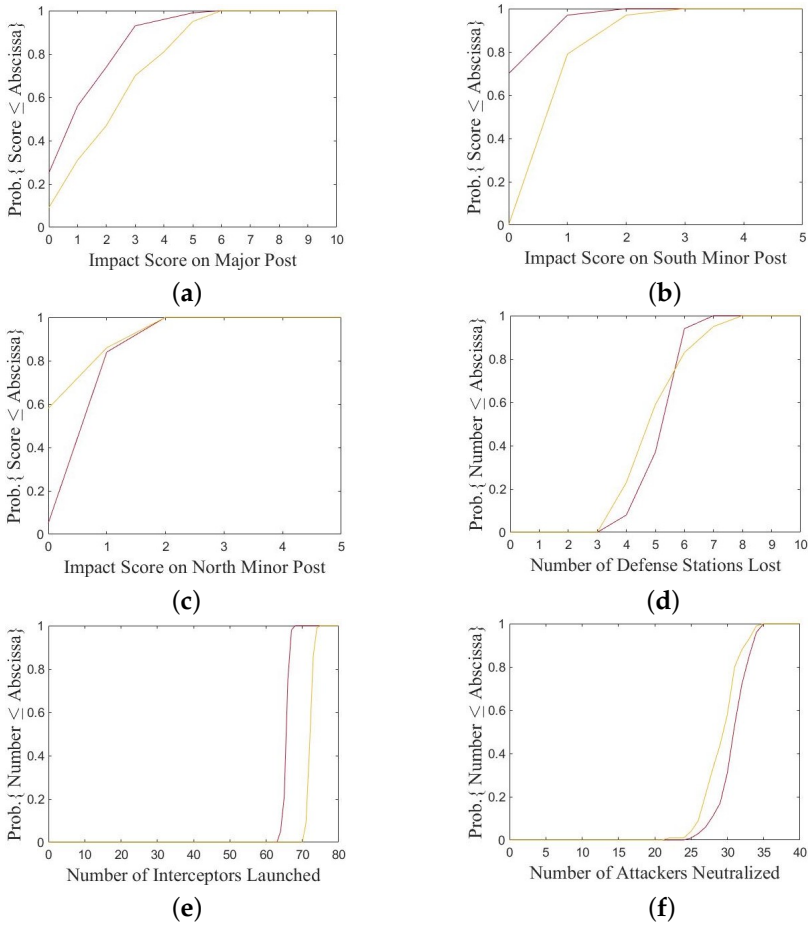

Figure 21. CDF of (**a**) impact score on major post; (**b**) impact score on south post; (**c**) impact score on north post; (**d**) number of lost defense stations; (**e**) number of launched interceptors; (**f**) number of lost attackers, against slant attack formation (brown) or pincer attack formation (yellow).

8. Conclusions

An aerial war game between an attack force and a roughly matched defense force has been designed and simulated. The goal of the defense force is to protect the assets by intercepting the approaching attackers, implemented with an optimal deployment plan of defense stations. Many practical factors have been incorporated into the game design, including large defense area and large number of agents, target assignment, interception, pursuer chasing evader, evading maneuvers, kill probability, flying range, impact radius, and so on. The deployment plan of defense stations is optimized with a PSO algorithm, based on four possible types of defense cost function. The simulation results are analyzed statistically and some interesting outlier cases are inspected. Rules of thumb for deploying defense stations have been summarized and used to form empirical deployment plans. The simulation results indicate that the optimal deployment plans outperform the empirical plans in protecting the major post and reducing the asset loss.

Author Contributions: Conceptualization, J.-F.K.; methodology, J.-F.K.; software, Z.-X.J.; validation, Z.-X.J. and J.-F.K.; formal analysis, Z.-X.J. and J.-F.K.; investigation, Z.-X.J. and J.-F.K.; resources, J.-F.K.; data curation, Z.-X.J.; writing—original draft preparation, Z.-X.J.; writing—review and editing,

J.-F.K.; visualization, Z.-X.J. and J.-F.K.; supervision, J.-F.K.; project administration, J.-F.K.; funding acquisition, J.-F.K. All authors have read and agreed to the published version of the manuscript.

Funding: This research received no external funding, and the article processing charges (APC) were funded by Ministry of Science and Technology, Taiwan, under contract MOST 109-2221-E-002-169.

Conflicts of Interest: The authors declare no conflict of interest

References

1. Zhang, G.; Li, Y.; Xu, X.; Dai, H. Efficient training techniques for multi-agent reinforcement learning in combat tasks. *IEEE Access* **2019**, *7*, 109301–109310.
2. Baspinar, B.; Koyuncu, E. Assessment of aerial combat game via optimization-based receding horizon control. *IEEE Access* **2020**, *8*, 35853–35863.
3. Zhang, H.; Huang, C. Maneuver decision-making of deep learning for UCAV through azimuth angles. *IEEE Access* **2020**, *8*, 12976–12987.
4. Liang, L.; Deng, F.; Lu, M.; Chen, J. Analysis of role switch for cooperative target defense differential game. *IEEE Trans. Autom. Control* **2021**, *66*, 902–909.
5. Garcia, E.; Casbeer, D.W.; Fuchs, Z.E.; Pachter, M. Cooperative missile guidance for active defense of air vehicles. *IEEE Trans. Aerosp. Electron. Syst.* **2018**, *54*, 706–721.
6. Singh, S.K.; Reddy, P.V.; Vundurthy, B. Study of multiple target defense differential games using receding horizon-based switching strategies. *IEEE Trans. Control Syst. Technol.* 2021, *early access*.
7. Li, Q.; Yang, R.; Feng, C.; Liu, Z. Approach for air-to-air confrontment based on uncertain interval information conditions. *J. Syst. Eng. Electron.* **2019**, *30*, 100–109.
8. Ma, Y.; Wang, G.; Hu, X.; Luo, H.; Lei, X. Cooperative occupancy decision-making of multi-UAV in beyond-visual-range air combat: A game theory approach. *IEEE Access* **2020**, *8*, 11624–11634.
9. Gao, K.; Yan, X. Study on the optimal strategy of missile interception. *IEEE Access* **2021**, *9*, 22239–22252.
10. Gao, C.; Kou, Y.; Li, Y.; Li, Z.; Xu, A. Multi-objective weapon target assignment based on D-NSGA-III-A. *IEEE Access* **2019**, *7*, 50240–50254.
11. Fonod, R.; Shima, T. Blinding guidance against missiles sharing bearings-only measurements. *IEEE Trans. Aerosp. Electron. Syst.* **2018**, *54*, 205–216.
12. Fu, H.; Liu, H.H.-T. Guarding a territory against an intelligent intruder: Strategy design and experimental verification. *IEEE/ASME Trans. Mechatron.* **2020**, *25*, 1765–1772.
13. Shishika, D.; Paulos, J.; Kumar, V. Cooperative team strategies for multi-player perimeter-defense games. *IEEE Robot. Autom. Lett.* **2020**, *5*, 2738–2745.
14. Salmon, J.L.; Willey, L.C.; Casbeer, D.; Garcia, E.; Moll, A.V. Single pursuer and two cooperative evaders in the border defense differential game. *J. Aerosp. Info. Syst.* **2020**, *17*, 229–239.
15. Fan, D.D.; Theodorou, E.; Reeder, J. Model-based stochastic search for large scale optimization of multi-agent UAV swarms. *arXiv* **2018**, arXiv:1803.01106.
16. Lee, G.T.; Kim, C.O. Autonomous control of combat unmanned aerial vehicles to evade surface-to-air missiles using deep reinforcement learning. *IEEE Access* **2020**, *8*, 226724–226736.
17. Wei, X.; Yang, L.; Cao, G.; Lu, T.; Wang, B. Recurrent MADDPG for object detection and assignment in combat tasks. *IEEE Access* **2020**, *8*, 163334–163343.
18. Hu, Q.; Han, T.; Xin, M. New impact time and angle guidance strategy via virtual target approach. *J. Guidance Control Dyn.* **2018**, *41*, 1755–1765.
19. Wei, X.; Yang, J. Optimal strategies for multiple unmanned aerial vehicles in a pursuit/evasion differential game. *J. Guidance Control Dyn.* **2018**, *41*, 1799–1806.
20. Pachter, M.; Moll, A.V.; Garcia, E.; Casbeer, D.; Milutinovic, D. Cooperative pursuit by multiple pursuers of a single evader. *J. Aerosp. Inf. Syst.* **2020**, *17*, 371–389.
21. Kennedy, J.; Eberhart, R. Particle swarm optimization. In Proceedings of the IEEE International Conference on Neural Networks (ICNN), Perth, WA, Australia, 19–24 July 2020; pp. 1942–1948.
22. Cheng, Z.; Li, F.; Zhang, Y. Multi-agent decision support system for missile defense based on improved PSO algorithm. *J. Syst. Eng. Electron.* **2017**, *28*, 514–525.
23. Liu, S.; Huang, F.; Yan, B.; Zhang, T.; Liu, R.; Liu, W. Optimal design of multimissile formation based on an adaptive SA-PSO algorithm. *Aerospace* **2022**, *9*, 21.
24. Zhong, W.J.; Li, X.B.; Chang, H.T.; Liang, F. Design of air defense deployment optimization model based on adaptive nested PSO algorithm. In Proceedings of the 2021 2nd International Conference on Intelligent Design (ICID 2021), Xi'an, China, 19 October 2021; pp. 172–177.